



Transport mechanisms of particulate emissions from artificial marine structures – A review

Niklas Czerner^{a,*}, Christian Windt^a, Nils Goseberg^{a,b}

^a Technische Universität Braunschweig, Leichtweiß-Institute for Hydraulic Engineering and Water Resources, Dept. of Hydromechanics, Coastal and Ocean Engineering, Beethovenstr. 51a, Braunschweig, 38106, Germany

^b Coastal Research Center, Joint Research Facility of Leibniz Universität Hannover and Technische Universität Braunschweig, Merkurstr. 11, Hannover, 30419, Germany

ARTICLE INFO

Keywords:
Offshore wind
Emissions
Particles
Fate
Transport

ABSTRACT

A vast number of artificial marine structures are currently installed offshore, and the rate of new installation is increasing. Especially offshore wind farms, a sub-type of artificial marine structures, are expected to grow significantly due to ambitious installation targets from international decision-makers. With increasing numbers of installed artificial marine structures, an assessment of possible adverse effects is more important than ever. To improve the environmental friendliness of artificial marine structures, an in-depth assessment of the transport and environmental fate of particle emissions is needed. The present work provides an overview of the involved processes of particle transport in the marine environment using the example of an offshore wind turbine. In this work, a first estimation on emission quantities is given for particulate emissions from marine structures, from which it is evident that emissions will increase in the next years due to an increasing number of marine structures.

1. Introduction

Thousands of artificial marine structures (AMS) are built in the marine environment, which are used for aquaculture purposes, oil and gas extraction through offshore platforms or for the generation of electricity from offshore wind farms (OWFs) (Gourvenec et al., 2022). In the next years and decades, the number of AMS will increase significantly, due to the ambitious expansion of offshore wind. At the end of 2023, a total capacity of 75 GW was installed globally, with much more to come (Global Wind Energy Council, 2024). It is expected that the annually installed power in offshore wind will steadily increase up to 30 GW^a in 2027 (IEA, 2022). Therefore, it is expected that the installed capacity in offshore wind will surpass 400 GW by 2033 (Global Wind Energy Council, 2024). A closer look at the ratio of offshore wind installations compared to oil and gas installation further underlines the importance of offshore wind: In 2020, 363 oil and gas installations were commissioned in European waters, whereas a total of 5402 grid connected wind turbines were operating in the same year in Europe (Wind Europe, 2021; European Commission, 2022). Additionally, new technologies like wave or tidal energy conversion are emerging, which will add to the number of AMS alongside the already existing structures (Clemente et al., 2021; The SET, 2022; Shetty and Priyam, 2022; Korte et al., 2024).

Furthermore, important transport routes traverse the oceans, leading to significant ship traffic in offshore areas (Sardain et al., 2019). While AMS will remain an important factor for human prosperity and a source for economic growth, the impact of those structures and vessels on the marine environment must not be neglected. In an evaluation of the severity of environmental impacts from AMS on the oceans, introduction of pollution was ranked as one of the most severe effects of AMS on the environment (Knights et al., 2024). One widely overlooked aspect of pollution originating from AMS is the effect of corrosion protection systems on the environment, just recently put into a broader focus by Kirchgorg et al. (2018) and Turner (2021). In recent literature, investigations on possible adverse effects of solute pollutants from galvanic protection can be found (Reese et al., 2020; Ebeling et al., 2023); however, the influence of particle emissions on the marine environment is still not thoroughly investigated. A significant part of a high-performance corrosion protection system for an AMS is a multi-layer coating, commonly built from epoxy resins and polyurethane (Momber and Marquardt, 2018), which can detach due to environmental factors, handling issues, or poor planning (Momber, 2016). Although this problem has not drawn much attention in the research communities yet, the whole scope of the problem is larger than expected. A recent report on the contribution of paint to the global

* Corresponding author.

E-mail address: n.czerner@tu-braunschweig.de (N. Czerner).

<https://doi.org/10.1016/j.marpolbul.2025.117728>

Received 9 September 2024; Received in revised form 20 February 2025; Accepted 20 February 2025

Available online 9 March 2025

0025-326X/© 2025 The Authors. Published by Elsevier Ltd. This is an open access article under the CC BY license (<http://creativecommons.org/licenses/by/4.0/>).

microplastic (MP) emissions has shown that the paint sector is the largest contributor to marine MPs, with approximately 1.9Mta^{-1} of MPs leaked into oceans and waterways (Paruta et al., 2021). On a larger scale, however, the emissions are not only resulting in microplastics, but also meso- and macro-plastics, as particulate emissions from AMS will not necessarily directly result in particles smaller than 5 mm, and breaking down into finer fractions may only happen over significant amount of time in the marine environment. A report from the *Earth Action* estimated that 40 % of all paint emissions at sea are released as macroplastic. Additionally, the report states that from the total amount of emitted paint, 18 % are released directly at the sea, e.g., through wear of ship hulls, AMS coatings, or the maintenance thereof (Paruta et al., 2021). The coatings contain a broad mixture of organic compounds, e.g., bisphenol A, which can possibly leak into the water (Kirchgeorg et al., 2018). Bisphenol A is an endocrine disruptor, which can lead to several diseases and impair fertility in animals and humans (Machtinger and Orvieto, 2014). Furthermore, Bisphenol A can accumulate in marine wildlife even at low concentrations (Paolella et al., 2024). Apart from bisphenol A, epoxy resin coatings were found to leak 4-tert-butylphenol into the surrounding water, which is toxic to marine organisms (Bell et al., 2020). Another group of harmful substances are heavy metals that can leak from anti-fouling paints commonly used on ships and in aquaculture (Kang et al., 2023; Castritsi-Catharios et al., 2015). One of the metals emitted is copper, which is toxic to fish (McIntyre et al., 2008). Since paint emissions at sea are a significant driver of anthropogenic impacts on the hydrosphere, the fate and transport of particulate AMS emissions needs to be investigated thoroughly, especially in the light of the rapid expansion of marine renewable energy generation in the next years. To the best of the authors' knowledge, the emitted quantities of particulate emissions from AMS are still unknown to this day, which is why a better understanding of the environmental fate and transport of the particles can aid to identify possible accumulation hotspots to better assess emission quantities. From there on, useful mitigation measures can be applied. An overview of the origin, fate, and transport of particulate AMS emissions, as well as the involved processes, are shown in Fig. 1. Pertinent literature was reviewed to identify important transport mechanisms. The scope of this work lies on particle emissions from the structures themselves, e.g., surface coatings. Particle emissions from the operation of the structures, such as particulate matter from combustion engines or operational fluids, are deliberately

excluded from this review, as well as solute chemical emissions. The transportation pathways of particulate emissions are presented and discussed at the example of an OWF, due to the enormous expansion of offshore wind in the next decades.

1.1. Objectives

This work presents an important first step towards a better understanding of the transport and fate of particulate AMS emissions, for which OWFs are used as a case study. With a focus on particulate offshore emissions, a large variety of involved processes are discussed, for example hydrodynamic transport in the water column, morphodynamic transport and mixing processes at the sediment bed, and the effect of biota on particle transport. The main objectives of this work are to:

- Provide a comprehensive overview of particulate emissions originating from offshore structures, from potential sources to potential sinks.
- Identify and discuss important particle transport processes.
- Identify knowledge gaps and give suggestions for future research.
- Give a first estimation on emission quantities.

1.2. Structure of this work

The remainder of this work is organised as follows: The used methods and materials of this work are described at the beginning of the corresponding sections. The processes related to particle emissions and transport are presented and discussed in the order in which they would naturally occur, i.e., from initiation of the emissions to final sink. At the end of each section, a discussion on the identified knowledge gaps is included. Following this logical order, particle emission sources are discussed in Section 2.1. Emissions from corrosion protection coatings are considered, as well as particulate emissions from the rotor blades, falling off into the water. In Section 2.2, the sinking of detached particles is discussed and influencing parameters like waves and currents are discussed. Section 2.3 treats the remobilisation of particles that reside on the sediment-water interface. Additionally, the influence of flow field around a marine pile foundation is discussed. In Section 2.4 the effects of weathering and marine organisms in general on the distribution and fate of waterborne particles are discussed. In Section 2.5 possible mechanisms for a particle transport over longer distances are discussed, and

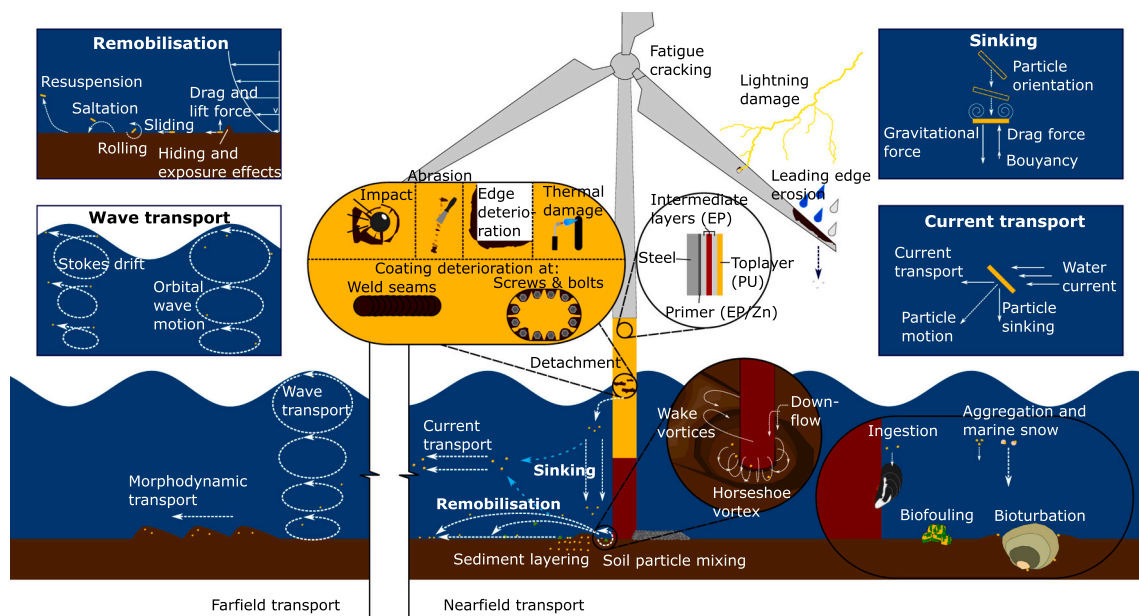


Fig. 1. Overview of possible transport pathways of particulate OWF emissions.

possible sinks are identified. Afterwards, a first estimation on the emission potential of coating emissions is given in Section 3. Finally, Section 4 concludes the paper and briefly summarises the most important task for future research, based on the previously identified knowledge gaps.

2. Literature review

A scoping literature research was conducted using the research databases *Scopus*TM and *Google Scholar*; once search results were obtained, these were sorted by relevance. In this context, we acknowledge that recent research by Ferreira et al. (2023) now stipulates to use multiple research databases in parallel, as search results amongst the three main search engines (*Scopus*, *Web of Science* and *Google Scholar*) differed significantly, with the third large database *Web of Science* having the highest ratio of irrelevant returns for an exemplary search string from the field of aquatic science. This finding contrasts earlier comparative work, looking at the database version of 2008 in which a large agreement between search results was confirmed (Archambault et al., 2009). Broad search terms were needed to find related publications, since exclusion of search terms multiple times led to very few results. To find the publications with the largest overlap with the topic of this work, the results were then manually assessed. For the sake of completeness, the thought process behind the literature research is explained here. To get a first overview over the topic, a first literature review was conducted, using the following keywords: *offshore*, *wind*, *structure*, *emission*, *coating*, *damage*, *transport*, *environmental fate*, *leading edge erosion*. There are a lot of publications related to offshore wind (e.g., 19.300 results in *Google Scholar* for *offshore AND wind AND coating AND emissions* on 10.07.2024), but most of the publications are either targeting the material science behind offshore coatings, or other emissions from OWFs, e.g., carbon dioxide within the production or lifetime cycle of structures, or noise as being emitted while structures are installed. With the collected information on the material properties for organic coatings, it was apparent that the emitted particles are negatively buoyant and part of the MP contaminating the oceans. Therefore, the keywords *microplastic*, *particle*, *settling*, *sinking*, *velocity*, *remobilisation*, and *incipient motion* were assessed next. To investigate the transport around a marine pile and in the sediment, the keywords *horseshoe vortex* and *sediment transport* were also included in the search. The research on particle transport revealed that organisms can also have a significant impact on the environmental fate of particles, which is why the terms *biofouling*, *marine snow*, and *bioturbation* were also assessed. The literature review was conducted in multiple searches with different search strings, which can be found together with the corresponding number of results in the Appendix (Appendix A). For searches with more than 100 results, the first 100 results per search, sorted by relevance, were analysed based on their title. From there on, 222 publications were further assessed by the content of their abstracts. Publications were analysed completely, looking at the full texts, when either information about (i) coating specifications, (ii) coating emissions, (iii) transport mechanisms, or the (iv) environmental fate of particulate matter were given. This manual filtering approach left 97 publications which were analysed in their entirety, and the findings of these publications are presented and discussed in this work.

2.1. Emission sources

To get a first impression of particulate emissions from AMS, possible particle sources, as well as the associated material composition, which is an important parameter for the transport of the emitted particles, are discussed in the following section.

2.1.1. Organic coatings

To protect offshore wind structures against corrosion damage, different strategies are chosen depending on the type of environmental

exposure the structure needs to endure. For the structural parts that are never submerged in water, ISO 12944-2 defines atmospheric corrosion as a process initiated by a thin film of moisture which can be enhanced by high relative humidity, condensation, and atmospheric pollution through deposition of reactive compounds on the substrate (ISO 12944-2, 2017). For steel structures with direct water contact, ISO 12944-2 defines three exposition zones, which are illustrated in Fig. 2 (ISO 12944-2, 2017):

- Underwater zone, which is below low tide water levels and thus permanently submerged in water.
- Intermediate zone, which is influenced by the tidal cycle or artificial effects. It ranges from low tide to high tide water levels and is subject to cyclic wetting and drying.
- Splash zone, which is subject to wave attack and spray deposition of ocean water. The splash zone extends to the height which is still reached by the spray from the colliding waves. Extreme corrosive stresses prevail in the splash zone due to wetting and drying and salt deposition.

Depending on the exposure zone, different coating specifications are given to achieve the best corrosion protection for the given exposure type. According to ISO 12944-2, the OWF parts which are not in direct contact with water for a prolonged amount of time are categorised in the corrosion category *CX* for extreme corrosive offshore environments and the submerged parts are classified in the category *Im4* for permanently in saltwater submerged structures with cathodic protection (ISO 12944-2, 2017). Due to wetting and drying, structures in the intermediate zone and the splash zone are categorised as a combination of *CX* and *Im4* (ISO 12944-9, 2018). To withstand the corrosive stress in the chemically aggressive marine environment, commercial OWFs are commonly coated with resin coating systems built from multiple layers of epoxy resin, covered by a polyurethane topcoat (Olajire, 2018). To ensure a sufficient adhesion of the coating system to the metal substrate, priming

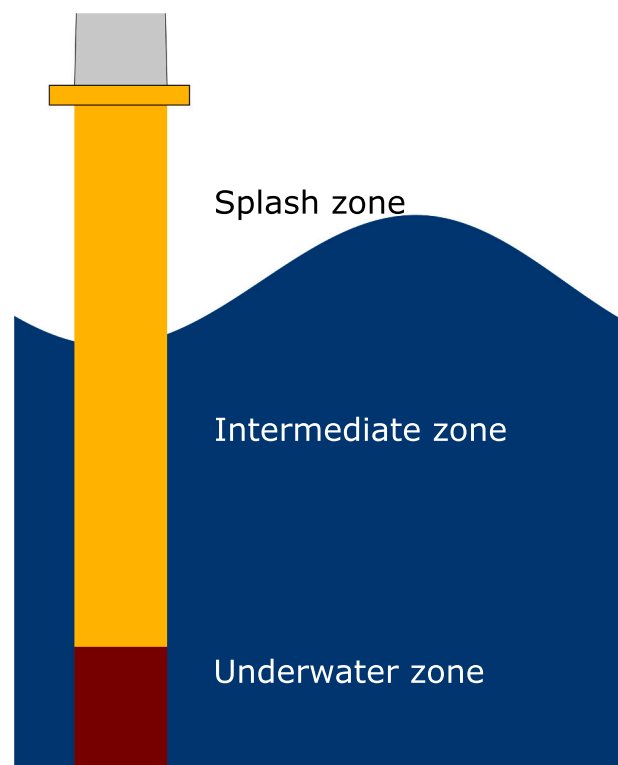


Fig. 2. Exposure zones for an offshore structure according to ISO 12944-2 (2017).

coats are applied. These priming coats are made from epoxy, zinc rich epoxy, or spray metal (Momber and Marquardt, 2018). Other applications for metal coatings are coatings for flange connections, frames, and railings; but organic coatings are the most commonly used coating systems overall (Momber and Marquardt, 2018). Coatings in the submerged zone are either applied as a thick single layer coating with a nominal dry film thickness (NDFT) of at least 800 μm or as two-layered coatings with a total NDFT of 350 μm or more. In the alternating water zone with a lot of wetting and drying cycles, coatings are applied with minimum two layers and a NDFT of a least 450 μm . In the atmospheric zone, coatings are built from multiple layers with a NDFT of 280 μm or more (ISO 12944-9, 2018). More information on coating specifications for NDFTs and amount of coating layers for structures exposed to offshore environments can be found in international standards, for example in ISO 12944-9 (2018). The summation of dry film thicknesses of all relevant coating layers gives a first indication as to how thick particles from marine coating released into the marine environment could potentially be, ranging from several micrometers for detaching of single coating layers up to almost a millimetre for detachment of a whole multi-layered coating system.

The aforementioned organic coatings are also applied to marine structures built from reinforced concrete. Reinforced concrete structures can be seriously damaged through corrosion of the reinforcing steel when built in the marine environment (Zheng et al., 2020). The porous concrete is exposed to high chloride ion concentrations and carbon dioxide, which enter through diffusion and lead to a depassivation of the reinforcement (Rodrigues et al., 2000). Coatings can delay the chloride intake and increase the time until corrosion initiation, with aliphatic acrylic and polyurethane coatings being the most effective in doing so (Sadati et al., 2015). Additionally, coatings from Polyurea are currently tested as surface coatings for marine concrete due to their high durability and low toxicity (Shojaei et al., 2021).

2.1.2. Coating failure mechanisms

Approximately 40 % of all paints leak into the environment due to mismanagement (Paruta et al., 2021). Research on ship hull coatings has shown that shipyards are significant point sources for particulate emissions, due to regular dry-docking and maintenance of the ships. Due to spray painting application or mechanical abrasion, e.g. sanding, coating particles are emitted in shipyards, where ship maintenance is conducted (Song et al., 2015; López et al., 2023). Through hull maintenance, ultrafine particles are released into the air when the coatings are abraded (López et al., 2022). A single boatyard can contaminate an area of approximately 12.000 m^2 (Eklund et al., 2014). OWFs are not regularly re-coated, which is why coating emissions are not as severe as shipyard emissions. However, coating losses directly at sea enter the oceans right away, whereas maintenance emissions from shipyards can be mitigated with a proper waste management. Possible reasons for coating losses directly at sea will be discussed in the remainder of this section.

During the operation of an OWF, the coating applied to the foundation of the structure will be subject to harsh environmental conditions in a highly corrosive environment, which can lead to delamination of the material due to coating failure. Momber (2016) collected data from operating OWFs to assess common failure mechanisms of corrosion protection systems. An overview over the most common coating failures is given in Fig. 3.

The most common failure mechanism are mechanical damages to the coating due to impacting or abrading forces. Another common coating failure is caused by wrong design decisions, for example, when bi-metal corrosion at non-isolated bolts or screws occurs underneath the applied coating. To ensure a sufficient coating adhesion, weld seams, and sharp edges need to be prepared accordingly. Weld seams need a high quality surface preparation by cleaning and grid blasting, whereas sharp edges need to be rounded off for the coating to adhere properly. Are these surface preparations omitted in the manufacturing process chain, the

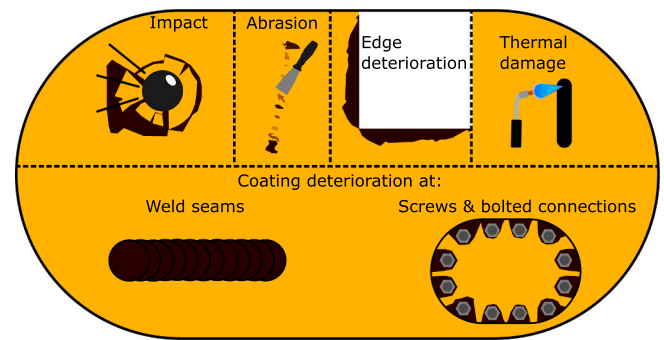


Fig. 3. Overview over the most common coating failure mechanisms occurring at OWFs, reported by Momber (2016).

coating has an increased chance of failure during the OWF lifetime. Finally, the coating can get damaged when thermally stressing work like welding is done on already coated parts, as hot debris gets incorporated in the coating surface.

When marine structures are exposed to the marine environment, organisms will settle on the surface of the structures (van der Stap et al., 2016; Pedersen et al., 2023; Isbert et al., 2023). Marine organisms exhibit a vertical zonation with a barnacle-dominated intertidal zone, followed by a mussel-dominated shallow subtidal zone and domination of anemones and filter feeding amphipods in the deeper subtidal zone (de Mesel et al., 2015). Additionally, the biofouling community changes continuously with time through factors like succession and predation (Zupan et al., 2023). Biofouling can alter the surface of steel substrates and lead to pitting corrosion or enhanced corrosion through removal of the passive oxide layer on the steel surface (Videla and Characklis, 1992). In the past, several adverse effects of biofouling on the functionality of marine structures and ships have been reported: Biofouling largely increases drag on ship hulls, increasing the shaft power at cruising speed up to 86 % (Schultz, 2007). In the context of AMS, it was found that marine growth increases drag on the foundations, leading to additional loads on the structures through currents and wave attack (Klijnstra et al., 2017). The protective function of the corrosion protection systems of offshore structures are not compromised by biofouling (Erdogan and Swain, 2021), but for impressed current protection biofouling can increase the current demand of structures in order to maintain a sufficient corrosion protection (Wang et al., 2018). In experiments on weathering of OWF corrosion protection coatings, it was shown that biofouling does not weaken the integrity of the investigated coatings (Momber et al., 2015). Although biofouling does not weaken the coating on a structural level, it might promote coating detachment through the additional loads on the biofouled surface. The aforementioned damage mechanisms cover the detachment of coatings applied to the steel structures of an offshore wind turbine (OWT), namely the foundation, transition piece, and tower. Common damages to the rotor blades of OWTs are reviewed in the following.

2.1.3. Emissions from turbine blades

To save as much weight as possible while still maintaining a high degree of stiffness, modern wind turbine blades are typically built from a polymer matrix reinforced with either glass or carbon fibre (Greaves, 2020). Glass fibre reinforced plastics are more common due to lower costs compared to carbon fibre reinforcements. In the past, the turbine blades were built with a polyester matrix, which is nowadays superseded by epoxy resins (Greaves, 2020). To protect the rotor blades against environmental stresses, a gelcoat or paint, often made from epoxy or polyurethane, is applied with dry film thicknesses of up to 800 μm (Kjærside Storm, 2023). Depending on the site specific conditions, a suited finishing layer is chosen depending on coating hardness and impact resistance. Harder coatings often show good impact resistance, whereas softer coatings, like polyurethane, protect the underlying layers

via impact absorption. Additionally, protection can be applied as tape to specifically protect the leading edge of the rotor (Kjærside Storm, 2023). However, due to the multitude of stresses acting on a rotor blade, it is not possible to protect it completely from degradation over its whole lifespan.

During operation, rotor blades are exposed to impacting raindrops, hailstones, and dust particles, which can damage the rotor blade over time. The so-called leading edge erosion occurs due to impacts of the small particles or droplets, mostly at the tip of the leading rotor edge. The rotor tip can reach speeds up to 100 ms⁻¹ leading to high local stresses on the rotor material upon impact (Greaves, 2020). Brittle surface materials can take direct damage from single droplet impacts, whereas softer materials do not get damaged by single droplet impacts. However, under repeated impacts both material types are likely to erode (Slot et al., 2015). Overall, the leading edge erosion commences in three stages (Amirzadeh et al., 2017). During the first stage, the incubation period, the rotor edge experiences no observable damages. The incubation period is followed by an increasing period in which the mass loss on the rotor edge starts and accelerates until the last period, the placid period, is reached in which the mass loss declines again (Amirzadeh et al., 2017). In general, the severity of the leading edge erosion heavily depends on the local climate conditions, such as frequency of rainfall and hailstorms, as well as the prevailing droplet sizes during these events and the rotor tip speed (Herring et al., 2019). Additionally, leading edge erosion is a problem that can occur early in the operating phase of an OWT. Reports from wind turbine quality assurance have shown that leading edge erosion typically occurs as early as three years after turbine operations started (Rempel, 2012). In addition to the occurring leading edge erosion, birds collide with wind turbine blades, which can cause a cracking of the gelcoat (Shohag et al., 2017). The collision of birds can possibly increase the number of emitted particles as the cracks are weak points in the surface which can deteriorate and ultimately cause delamination (Shohag et al., 2017).

Apart from blade erosion, lightning strikes can damage the rotor blades of wind turbines or even lead to complete failure of the blades (Yokoyama, 2013). Although there are lightning protection measures taken to reduce the probability of a lightning strike, such events still do occur as they cannot be mitigated completely (Yasuda et al., 2012). Structures such as OWTs are tall structures with large rotating parts, which might increase the probability of lightning discharges on OWTs in a way that multiple discharges on singular structures during a single storm appear realistic (Rachidi et al., 2012). Lightning damages can lead to delamination of the surface layer of the rotor blade due to the high temperatures during a lightning strike. In more severe cases, lightning strikes can cause debonding of the rotor shells (Yasuda et al., 2012). Modern rotor blades are built from two shells, which are joined along the edges and supported by internal beams (Greaves, 2020), which can lead to a detachment of the rotor tip. The most severe lightning damage occurs when the lightning can enter the rotor blade and heats the air inside. Due to thermal expansion of the entrapped air, the whole rotor blade can shatter (Yasuda et al., 2012).

Another possible entryway for particles from OWTs to the environment is fatigue cracking (Samborsky et al., 2008). The cyclic motion of the rotor and forces exerted by winds can lead to stresses that concentrate at the root of the rotor blade. Fibre reinforced composites can delaminate under these conditions (Samborsky et al., 2008), which might lead to particles entering the environment or even failure of the whole blade in severe cases. Apart from the rotor blade, fatigue cracking can also occur on heavily stressed parts of the OWT steel structures (Adedipe et al., 2016), leading to possible attack points for corrosion and thereby promoting delamination of coating material.

All in all, several possible sources for particle emission can be found at an OWF; however, to date, a lot of involved parameters remain unknown.

2.1.4. Knowledge gaps

As can be seen from the review in Sections 2.1.1 and 2.1.3, there are some particles detaching from OWFs, which will enter the environment during the operation period. In the case of delaminating coating (corrosion protection coating or blade gelcoat) one would expect flat and almost two-dimensional particles of various sizes and shapes, due to their thin dry film thickness in relation to the large area covered. However, there is, to the best of the authors' knowledge, no data available yet on exact quantities, size distributions, or shapes of detaching particles of any kinds in the context of OWF emissions, although there are reports on coating damages in the context of corrosion assessment (Momber, 2016). Additionally, the impact of wildlife on the coating emissions needs to be quantified further, as it is still unknown which influence bird collision or biofouling have on the emitted particle quantities (Verma et al., 2023). Therefore, more research on the properties of detaching particles is needed. Additionally, an investigation on the condition of the detaching particles can help to understand the degradation due to weathering and mechanical abrasion prior to detachment and might aid in finding suitable parameters for later simulations on the particle distribution.

Another interesting aspect worth investigating is the influence of the exposure regime during the operation on the material properties of the emitted particles. Coating specifications differ throughout the exposure zones (ISO 12944-9, 2018), introducing a variety of different thicknesses and material compositions of particles. Apart from different material compositions and thicknesses, weathering during the coating life will also influence the material properties and, ultimately, affect the environmental fate of emissions (Waldschläger et al., 2020). Coatings will weather differently, depending on the exposure they have to endure during operation. A more detailed discussion on the weathering of coatings can be found in Section 2.4. Possible transport pathways after detachment of the particles are discussed in the following.

2.2. Sinking

After detachment, the particles either enter the water by falling from the air into the water body, or they are already submerged, when a delamination or detachment from a rigid surface occurs underwater. In a next step, particles will sink towards the seabed, since densities of cured corrosion protection coatings and paints are higher than the surrounding seawater with a density range of approximately 1500 kg m⁻³ to 2000 kg m⁻³ (Turner, 2021).

In the first stage of sinking, the particle gets accelerated by the gravitational force, F_g (see Eq. (1)). During acceleration, the drag force, F_D (see Eq. (2)), increases, counteracting the gravitational acceleration until an equilibrium state is reached (Dietrich, 1982).

$$F_g = (\rho_s - \rho)gV \quad (1)$$

$$F_D = C_D \rho \frac{w_s^2}{2} A \quad (2)$$

In Eqs. (1) and (2), ρ_s is the density of the solid particle, ρ is the density of the ambient fluid, g is the gravitational acceleration, V is the particle volume, C_D is the drag coefficient, w_s is the particle settling velocity, and A is the projected area of the particle. At the equilibrium state, i.e., continuous, non-accelerated sinking, the drag coefficient C_D can be obtained by rearranging Eqs. (1) and (2):

$$C_D = \frac{2(\rho_s - \rho)gV}{\rho w_s^2 A} \quad (3)$$

As seen in Eq. (3), the drag coefficient C_D depends on the projected area of the particle to the flow. For spherical particles, the projected area does not change with particle orientation. For other particle shapes, though, the particle orientation during settling plays an important role for the settling behaviour. In this work, the focus is placed on particles originating from corrosion protection coatings of AMS, which will be

primarily flat and two-dimensional in shape due to the thin coating thicknesses (Momber and Marquardt, 2018). During sinking, flat particles will orient with the largest projected area perpendicular to the line of motion, maximising their drag (Stringham et al., 1969; Goral et al., 2023a). A schematic of a flat particle sinking undisturbed in a fluid is shown in Fig. 4. In addition to the particle geometry, the drag forces are also dependent on the prevailing flow regime, which can be categorised by the particle Reynolds number (Stiess, 2009), shown in Eq. (4).

$$Re_p = \frac{w_s d_p}{\nu} \quad (4)$$

In Eq. (4), ν is the kinematic viscosity of the fluid and d_p is a characteristic diameter of the investigated particle. For low particle Reynolds numbers ($Re_p < 0.25$) a laminar flow regime prevails, where viscous forces determine the particle drag. With an increasing Reynolds number, the influence of turbulence on particle drag increases as well. For $0.25 < Re_p < 10^3$, the particle drag is influenced by both viscous and inertial forces, leading to vortices and vortex shedding at the particle. For $10^3 < Re_p < 2 \cdot 10^5$ a fully turbulent flow emerges around the particle, which is mostly dominated by inertial forces.

In calm water conditions, the sinking of flat particles depends on their orientation, particles do not necessarily sink in a straight line of motion. Oscillating movement and tumbling of the particle can also occur (Stringham et al., 1969). During tumbling or other secondary motions, the settling velocity can vary, but often a stable settling position is reached after a short orientation period (Ahmadi et al., 2022). Stable sinking means in this regard that the terminal settling velocity remains mostly constant, while a certain degree of secondary movement can still occur (Ahmadi et al., 2022). The time elapsed until the final orientation is reached depends on the initial orientation of the particle (DiBenedetto et al., 2018). Numerical simulations with elliptical particles showed that for a particle entering the water perpendicular to its preferential orientation, most of the re-orientation will happen during the first 20 s (DiBenedetto et al., 2018). The effect of the particle shape poses a problem for an accurate but general prediction of settling velocities, since most equations were developed for spherical particles or sediment particles; many of them lack accuracy when transferred to diversely shaped particles like microplastics (MPs) (Waldschläger and Schüttrumpf, 2019a). In the recent literature, several studies aim to find more accurate equations that predict the sinking of either natural or MP particles of various shapes and sizes (e.g. (Goral et al., 2023a; Waldschläger and Schüttrumpf, 2019a; Francalanci et al., 2021)). A recent study by Goral et al. (2023a) presents a shape-by-shape approach, leading to different parametrisations for C_D for different particle shapes. For flat particles at Reynolds numbers $> 2 \cdot 10^2$, C_D was found to be

constant at $C_D = 1.12$ for disks and $C_D = 1.23$ for square plates (Goral et al., 2023a). The aforementioned investigations examined the sinking behaviour of virgin particles without the effect of weathering or biofilm growth on the particles. Weathering and biofilm growth can influence the settling of particles as well and is further discussed in Section 2.4. Additionally, particle aggregation and marine snow also influence the settling of particles and are further discussed in Section 2.4.1.

2.2.1. Horizontal sinking components

The aforementioned principles on particle settling consider at this point only a particle sinking in a fluid at rest with zero ambient flow field, which does not properly represent the complexity of offshore environments. Waves and currents impose significant ambient flow fields, influencing the transport of the coating particles. Shear forces and pressure gradients induced by waves act on the particle orientation, which ultimately influences the settling velocity of the particle (DiBenedetto et al., 2019). Stronger wave influence leads to greater disturbance of the preferred settling orientation, with distinct, wave frequency-dependent particle motions; with decreasing wave orbital velocities and thus deeper submergence depths, particles return to the preferred undisturbed settling orientation. Additionally, wave induced shear forces can cause rotation of the sinking particle (DiBenedetto et al., 2019). Another effect caused by waves is the Stokes drift: A non-linear drift in the direction of the wave propagation, caused by the oscillating motion of the waves (Stokes, 1847). Stokes drift has a strong influence on the transport of buoyant particles in the upper water layer, but the Stokes drift decreases with increasing submergence depth as the orbital wave motion decreases as well. For instance, at a depth of 2 m, only 10 % of the Stokes drift remains of what occurs at the surface (Fraser et al., 2018). Therefore, the effect of Stokes drift on the settling particles will be small, since the particles remain in the upper water layers only for only a few seconds.

The waves and currents around OWFs introduce horizontal shear, which can result in horizontal transport of the particles during sinking (DiBenedetto et al., 2018). However, due to the high density of the organic materials, emitted particles are expected to sink to the seabed in the nearfield around the structure from where they detached, but currents might lead to a drifting of the sinking particles in the current direction. Additionally, currents also might influence the preferential orientation of the sinking particle, altering the transport distance and particle dispersion (DiBenedetto et al., 2019). Another flow related phenomenon which influences the settling and remobilisation of particles is the characteristic flow around a monopile structure, which is further discussed in Section 2.3.1.

2.2.2. Knowledge gaps

The investigation of MP particle transport has gained momentum in the scientific community, with several investigations on settling velocities for MP particles of various shapes and sizes, as well as their transport behaviour. Valuable implications for the sinking behaviour of OWF coating particles can be drawn from these publications, while distinct similarities or differences in shape, size and particle distributions need to be elaborated yet. A focus on tests with common coating materials like epoxy resin or polyurethane are still missing; these have different material properties from common MP materials, such as polyethylene terephthalate or polypropylene. It is therefore a promising endeavour for future research to conduct sinking tests with common coating materials to extend the existing database on particle sinking velocities with these newly-addressed materials. Additionally, it is of interest to validate the approach by Goral et al. (2023a) for even flatter particles than the ones investigated in their study, by conducting tests with particles above MP size but with the same thickness. Furthermore, the influence of currents on the orientation and velocity of settling particles need further assessment; this will target the question, whether currents have a significant impact on the spatio-temporal distribution of particles around a structure. Finally, the influence of ocean waves

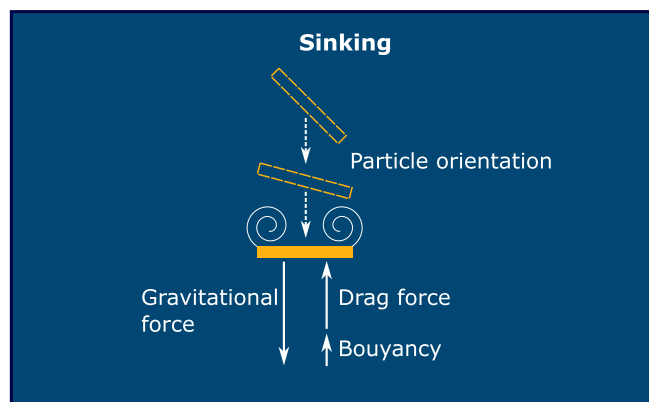


Fig. 4. Schematic of a flat particle sinking in the water column. The particle reorients itself during sinking to maximise the drag. The terminal settling velocity is reached once gravitational forces, buoyancy, and drag forces are in equilibrium.

should also be taken into account. Experiments with waves and currents in combination are expected to provide valuable insights on their influence on settling particles with high densities, such as those originating off coating materials.

2.3. Remobilisation

After the settling stage of particles that have been deposited on or mixed into the ocean bottom sediments, these particles remain mostly stationary until they potentially get remobilised, for example by strong flow fields as a result of storm or current action (Li et al., 1997). Research on MP particle transport in rivers has shown that, for instance, rainstorm events can trigger the remobilisation of MP particles due to increased current velocities during the storms (Ballent et al., 2013; Hurley et al., 2018). The general principles for remobilisation of particles were first studied for sediment transport (Ballent et al., 2013; Goral et al., 2023b; Waldschläger and Schüttrumpf, 2019b).

A flow near a wall can be divided in an inviscid outer flow, and a boundary layer close to the wall (Schlichting and Gersten, 2017). The flow in the boundary layer can be laminar or turbulent. With increasing roughness, the transition from laminar to turbulent boundary layer flow occurs at lower Reynolds numbers (Schlichting and Gersten, 2017). The boundary layer is important for transport processes, since waves and currents force water motion at the sediment bed and lead to sediment transport in the boundary layer (Afzal et al., 2021; Holmedal and Myrhaug, 2006). When waves approach the shoreline, transformation effects increase the skewness of the waves, leading to asymmetric waves which induce a net onshore transport of sediment (Salimi-Tarazouj et al., 2024). The sediment is mostly transported in the wave propagation direction, but when currents and waves occur at an angle relative to each other, the sediment transport decreases (Afzal et al., 2021).

The onset of transport for sediment particles can be described as a function of the critical Shields parameter θ_{crit} and the Reynolds number for grains (Shields, 1936). The critical Shields parameter can be expressed as follows:

$$\theta_{crit} = \frac{\tau_{crit}}{(\rho_s - \rho_f)gD} \quad (5)$$

In Eq. (5), τ_{crit} is the critical shear stress, ρ_s is the sediment density, ρ_f is the fluid density, g is the gravitational acceleration, and D is the particle diameter. The grain-dependent Reynolds number is defined as follows:

$$Re = \frac{v_* D}{\nu} \quad (6)$$

In Eq. (6), v_* is the friction or shear velocity and ν is the kinematic viscosity of the fluid.

Once the particles are in motion, different transportation modes occur: rolling, sliding, saltation, and resuspension (US Army Corps of Engineers, 2003). During rolling and sliding, the particles move on the sediment bed while maintaining ground contact. When saltation occurs, particles are lifted from the bottom but can not be retained in suspension for a longer time and settle again. Lastly, resuspension can occur, where particles are lifted from the sediment bed and are retained in suspension (Mazzuoli et al., 2022). A schematic of the remobilisation of a flat particle on a sediment bed is shown in Fig. 5.

In recent literature, MP particles were investigated in incipient motion experiments to gain more knowledge on the behaviour of MP particles on a sediment bed under the influence of currents (Ballent et al., 2013; Goral et al., 2023b; Waldschläger and Schüttrumpf, 2019b; Yu et al., 2022). Most MP particles are transported as bedload (Guler et al., 2022), with rolling, sliding, and saltation as main transportation modes (Waldschläger and Schüttrumpf, 2019b). Since the MP particles differ in size and shape from the background sediment repository, hiding-exposure effects play an important role in the particle transport (Waldschläger and Schüttrumpf, 2019b). On sediment beds with a larger

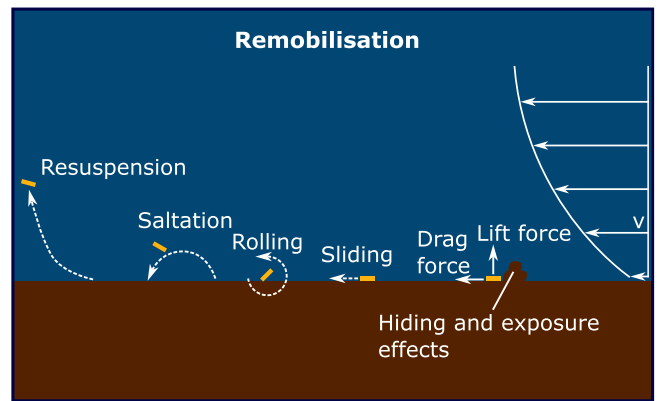


Fig. 5. Schematic of a flat particle on a sediment bed. If the critical shear velocity is exceeded, the particle gets remobilised and is transported again. The different transportation modes sliding, rolling, saltation, and resuspension can occur (not necessarily in that order).

median grain size, small particles can be shaded from the flow by larger sediment particles, leading to higher bottom shear stresses needed for a remobilisation of the MP particles. Vice versa, when larger particles lie on a finer sediment, the particles are more exposed to the flow, reducing the needed bottom shear for remobilisation. In bidirectional currents hiding and exposure effects can increase the erosion stability of the sediment bed due to bidirectional displacement and rearrangement of individual grains (Schendel et al., 2018). Another effect which might influence the transport of OWF particles is the formation of an armour layer. Investigations with wide graded sediments have shown that in unidirectional currents the fine graded sediment will wash out, leading to the formation of a stable armour layer (Schendel et al., 2016). It is still unknown, if coating particles get washed out with the fine sediment or are part of the armour layer formation. Another important parameter for the remobilisation of particles is the particle density. With increasing density the critical shear stress for incipient particle movement increases as well (Waldschläger and Schüttrumpf, 2019b). However, most MP particles are located beneath the classical shields curve on the shields diagram (Goral et al., 2023b), indicating that MP particles will get transported before the sediment erodes. In addition, the MP particles behave more like native sediment grains in the classical shields diagram, the closer the ratio of MP particle diameter to median sediment grain size is to 1 (Waldschläger and Schüttrumpf, 2019b). The classical shields diagram can be modified to predict the onset of transport of MP particles as well as native sediment particles, when static friction and hiding exposure effects are considered accordingly (Goral et al., 2023b). Another form of remobilisation is scour of sediment directly around the foundations of offshore wind structures, which is discussed in the following.

2.3.1. Flow around the foundation base

When a cylindrical structure like a monopile foundation is installed in the seabed, a characteristic, yet complex flow field emerges around the structure (Dargahi, 1989; Sumer et al., 1997; Chen Ong et al., 2017). When waves approach the marine pile, a characteristic horseshoe vortex emerges at the bottom of the foundation, which is heavily erosive and causes scour around monopiles (Nielsen et al., 2012). A characteristic flow field around a structure as a result of wave action in combination with a marine pile is shown in Fig. 6.

At the downstream side of the monopile vortices are shed (Sumer et al., 1997). This characteristic flow occurs around all monopile foundations regardless whether they are protected by scour protection or not. Even at foundations with an installed scour protection a sinking of scour protection due to erosion at the edges due to the horseshoe vortex were observed (Nielsen et al., 2012). Since the vortices are strong enough to

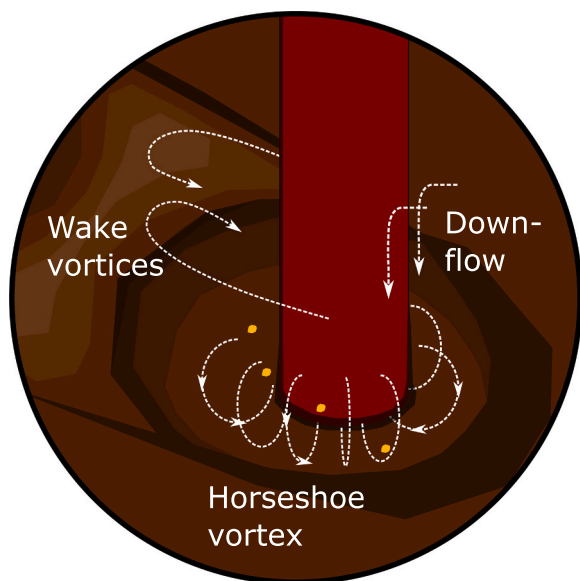


Fig. 6. Schematic of the flow around a cylindrical foundation at the seabed. At the front face of the pile a downward flow emerges. A horseshoe vortex forms around the cylinder at the bottom. Wake vortices form behind the structure.

carry sediment particles, they will also carry coating particles as they have a lower density than the sediment (Turner, 2021). Therefore, a mixing of soil and emitted particles at the bottom of monopile foundations can be expected with coating particles being incorporated into deeper sediment layers. However, around monopiles with scour protection, the particles potentially fall between protection elements (i.e., rock material) of the scour protection which could shield the particles from any horseshoe vortex induced displacement due to hiding effects (Waldschläger and Schüttrumpf, 2019b). Behind the marine pile, lee vortices have an impact on the transport of particulate matter in the vicinity of the offshore structure. The lee wake vortices are too weak to carry sediment (Nielsen et al., 2012) but lighter particles might get caught into the turbulent flow resulting from the vortices until they decayed to a distant point behind the marine pile where the particles settle again. Therefore, it is possible that particles accumulate on the sediment in the wake of a monopile.

2.3.2. Knowledge gaps

The review on the remobilisation processes of particles originating from coating systems used in regard to structures placed in the oceans has revealed various knowledge gaps: the coating particles are emitted from marine structures, which often times consist of circular piles, or jacket structures, build up from circular piles. The present review shows that very complex flow conditions prevail, which results in a yet unclear remobilisation potential of coating particles in the vicinity of marine structures. In that regard, a process that has not been investigated yet is the exact influence of the complex flow field around the foundation base on the distribution of particles, and their stratification behaviour when mixing into the background sediment depository. For a well-founded assessment of the environmental impact of coating emissions, it is important to know possible accumulation hot-spots as well as the transport pathways. Therefore, it is important to investigate the flow around the foundation in regard to its influence on the transport of particles and to assess, whether particles accumulate in the sediments around the foundation. Furthermore, the influence of a scour protection should be investigated to gain a comprehensive understanding of the involved processes in particle transport around marine foundations with scour protection. In the most recent publication, Goral et al. (2023b) investigated nine different regularly shaped and eight irregularly shaped particles. Most of the investigated particles have a diameter of 5 mm or

less, which is why they can be considered MPs. These investigations offer a valuable foundation for a further assessment of particulate emissions from OWFs as well. However, only 65 % of paint emissions are emitted as microplastic in the marine sector, the remainder is emitted as macroplastic (Paruta et al., 2021). From the images on coating damage provided by Momber (2016) it is apparent that coating damages are located in a range of a few millimetres up to several centimetres. There will also be emitted particles with a size well above 5 mm making it an important task for future investigations to confirm the findings of Goral et al. (2023b) for coating materials like epoxy resin and polyurethane coatings and to extend the database with larger particles above MP size. Furthermore, transport distances of emitted coating particles are still not quantified yet, which can help to assess the environmental impact of the AMS. Therefore, it is a promising task for future research to quantify transport distances in future investigations.

2.4. Influence of weathering and marine organisms on particle transport

Structures built in the harsh offshore environment will experience a multitude of environmental stresses, for example UV radiation from the sun and biofouling through marine organisms. An overview of the mechanisms by which marine organisms can influence the particle transport is provided in Fig. 7.

Coating and blade materials will experience environmental stresses, depending on the exposure of the material to stress factors like UV-radiation, mechanical stress or marine growth. A blade gelcoat will be subject to UV radiation but less influenced by marine biofouling unless it enters the seawater due to previous delamination. When exposed to UV-radiation for a longer period of time, the surface of the exposed material changes due to the formation of micro cracks (Rosu et al., 2005). Once degradation was initialised, the degradation can continue thermo-oxidative as a further degradation of material at moderate temperatures (Andrady, 2011). Particles weathered by UV-radiation are more brittle and break into smaller fragments due to mechanical stress (Andrady et al., 2022). Another instance of mechanical degradation occurs in high energetic environments such as the swash zone, where energy dissipation of breaking waves together with a strong mixing of particles and sediment leads to a breakdown of particles into smaller fragments (Efimova et al., 2018).

Materials submerged in water, on the other hand, will experience degradation through biofouling by marine organisms. Organisms settle on the surface of the polymer and change the mechanical and chemical properties of the fouled material (Muthukumar et al., 2011). In general, biofouling alters the surface of the particles, which is why particles with a large surface area to volume ratio (e.g. smaller particles) are more affected by biofouling (Chubarenko et al., 2016). The particulate OWF emissions covered in the present paper have a high density and will sink right after detachment, which directly influences the biofilm growth on the particles' surface. The growth of bio-active films on MPs depends on the radiation intensity of sunlight, which leads to seasonal growth

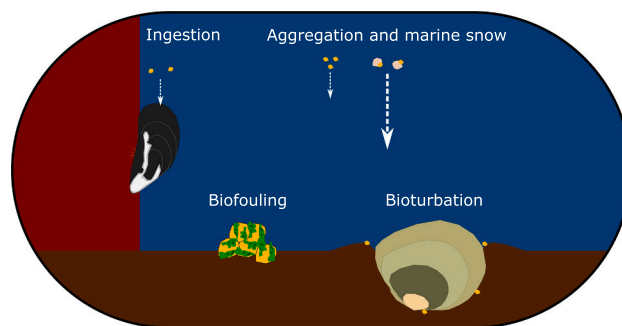


Fig. 7. Overview over the influence of marine organisms on the transport of particles in marine waters.

effects during seasons with high sunlight intensity, for example summer (Kaiser et al., 2017). Since sunlight intensity also decreases with increasing water depth, biofouling influences mostly the settling behaviour of particles near the water surface (Pedersen et al., 2023). Therefore, most of the biofouling will occur during the time when the materials are still attached to their respective structure. It was found that biofouling can increase the settling velocity of MP particles and can also cause buoyant particles to sink after they have been colonised by organisms (Kaiser et al., 2017). In total, the settling velocity increased up to 81 % after 6 weeks of exposure to biofouling. In a different test, Waldschläger et al. (2020) collected already weathered and fouled MP particles from a river environment. The authors found a slight decrease in settling velocities of biofouled particles, which was explained by an increased roughness and decreased density of the biofouled particles. Since biofouling composition is largely influenced by local factors such as sunlight intensity, geographical orientation, or depth (Pedersen et al., 2023), possible effects of marine organisms on the settling velocity of particles need to be investigated for site specific species. Additionally, biofouling communities exhibit a seasonality, with the highest abundances in summer and autumn and lowest abundances in winter and spring (Coolen et al., 2022). Another effect which influences abundance of species is the community age, which leads to a decrease in abundance with higher age (Coolen et al., 2022). Therefore, seasonality and structure age are also important factors to consider in future investigations.

2.4.1. Particle aggregation

Biological aggregation is an influential mechanism that effectively affects the settling of particles when bonded by biological matter, such as microorganisms and their associated by-products (Nguyen et al., 2020). Single particles as well as multiple particles can attach to a single piece of biological matter, forming aggregates. The aggregates often have irregular shapes and differ in density from virgin particles. It was found that aggregates have a 50 % slower sinking velocity, which increases the time of the vertical transport (Nguyen et al., 2020). The lower settling velocity could therefore increase the distance a particle travels before it reaches the sediment. Additionally, aggregation might also influence the remobilisation behaviour. Due to an increased surface area and a decreased density, it appears realistic that aggregation of particles with biological matter decreases the critical shear stress for remobilisation and thereby increases the mobility of aggregated particles.

A specialised form of aggregation is marine snow, which embraces aggregates formed from organic detritus, microorganisms, and clay materials (Allredge and Silver, 1988). Marine snow can increase the settling velocity of MPs by several orders of magnitude under laboratory conditions (Porter et al., 2018). However, the increase in settling velocity is significantly stronger for particles with low settling velocities, which would stay mostly afloat due to water and wave motion. Since most particles emitted from OWFs are expected to sink in the vicinity of the emission source, marine snow and aggregation might not have a large impact on the particle distribution.

2.4.2. Removal of particles from the water column by marine organisms

Apart from aggregation and biofouling, marine organisms can influence the particle transport through ingestion or burial. Filter feeding organisms like *Mytilus edulis* were found to ingest paint particles (Turner et al., 2009). A whole community of filter feeders at an OWT can potentially clear the water column up to 14 m around the foundation from all suspended food particles (Voet et al., 2022), which leaves the filter feeders at a high risk of ingesting microscopic particles which can originate from abrasion or leading-edge erosion. Macroscopic coating particles will not remain suspended in the water column for extended periods of time, due to the high density of the coating material, which reduces the potential time for ingestion by filter feeders, reducing the probability of ingestion. But not only filter feeders can ingest particles

from the water. Seabirds can also mistake floating plastic debris for prey (Provencher et al., 2014). However, direct ingestion of OWF particles through seabirds appears unlikely, since seabirds that feed at the water surface have the highest ingestion risk of plastics (Provencher et al., 2014) and OWF particles of a size which a seabird can visually detect will not stay afloat due to their high density. Ingested particles are removed from the water column and will no longer be directly affected by the transporting forces exerted by the water until the particles are excreted. Particle ingestion opens another transportation pathway of trophic transport through the food chain, when animals with ingested particles are eaten by predators (Nelms et al., 2018).

Marine organisms are not only at risk of ingesting particles. Benthic fauna, which move soils through bioturbation, was found to bury MP particles into deeper sediment layers which the particles would normally not reach (Näkki et al., 2017; Coppock et al., 2021). Burial depths of up to 10 cm could be observed (Coppock et al., 2021). The deeper burial of the particles in the sediment can hinder further transport of the particles, which is why the sediment bed acts as a sink for deeply buried particles (Coppock et al., 2021).

2.4.3. Knowledge gaps

With the increased attention on the environmental fate of MP particles, first investigations were conducted investigating the vertical transport of biofouled or aggregated particles (e.g. (Waldschläger et al., 2020; Kaiser et al., 2017; Nguyen et al., 2020)). In some cases, biofouling increased settling velocities whereas in other cases it leads to a decrease of the settling velocity, which indicates that the complex effects of weathering and biofouling can vary for different sites and materials. Therefore, it is important to investigate weathering and biofouling effects under site specific conditions. However, Waldschläger et al. (2020) provide an insightful discussion on the investigation of settling velocities for MPs and came to the conclusion to first investigate virgin particles and then later consider weathering and biofouling effects.

2.5. Far field transport and possible sinks

The transport mechanisms discussed in Sections 2.2 and 2.3 cover the main mechanisms which influence the distribution of particulate emissions in the vicinity of singular structures in an OWF. From there on, particles can get transported over longer distances by morphodynamic processes. In the transitional area between shallow and deep water, the orbital motion of the occurring waves influences the sediment and can lead to sediment transport at the seabed. Due to the circular orbital motion as a result of wave, two accelerating components exist: One in the direction of wave propagation and one in the opposite direction (Bijker et al., 1976). Depending on which acceleration dominates, the sediment gets transported in the respective direction. Additionally, the occurrence of secondary waves can lead to a sediment transport in opposite direction of the wave propagation direction (Bijker et al., 1976). Apart from waves, tidal currents also lead to sediment transport at the seabed (Schendel et al., 2018). In areas dominated by tidal currents, it was found that long term sediment transport is mostly driven by strong currents in combination with large waves with frequent occurrence. Although extreme events show a high probability for sediment transport, they are not the main driver for long term sediment transport due to their infrequent occurrence (Soulsby, 1987). The importance of waves on the bottom sediment transport decreases with water depth, as orbital velocities of the waves decline significantly with increasing depth (Soulsby, 1987). Since common MP particles begin to remobilise at lower critical shear stresses than natural sediment grains (Goral et al., 2023b) it appears realistic that particles entrapped in the sediment will get transported by the natural sediment movement as well. The transport of particles along with the sediment can be significantly influenced by tidal currents (Aldridge, 1997). Depending on the site, the ebb or flood current can be stronger due to a higher average magnitude or

higher peak current and ultimately result in a net transport in the dominant direction (Aldridge, 1997). The influence of tidal currents on the bottom shear stress is also dependent on the water depth, as maximum bottom shear stress in continental shelf areas is mainly dominated by major wind events and to a lesser extent by tidal currents (Hall and Davies, 2004). Therefore, a comprehensive knowledge of the bottom shear dominating currents around OWFs can help to identify important transport routes and find zones of low bottom shear where particles potentially accumulate.

Ultimately, particles can not only get transported over long distances with the sediment, the sediment can also be seen as the final sink of the emitted particles. First studies have shown that deep sea sediments act as a possible sink for negatively buoyant MPs (Woodall et al., 2014; Näkki et al., 2019). The particles sink to the seabed and get mixed into the sediment eventually. For a deep sea sediment at a continental shelf, MP particles were found at burial depths of up to 3.5 cm (Martin et al., 2017). As mentioned in Section 2.4.2, even deeper burial depths can occur in areas with a high bioturbation activity. Additionally, bioturbation does not lead to a digging up of already buried particles from the sediment (Näkki et al., 2019). Therefore, it is realistic that the OWF particles will ultimately end up in the sediment after transportation through the previously explained mechanisms.

2.5.1. Knowledge gaps

The sediment was identified as the final sink for negatively buoyant particle emissions. However, there are still some unknown factors, for example how long it will take a particle to end up being mixed into the sediment. Furthermore, it is still unknown if accumulation hot-spots exist in the sediment and under which conditions they possibly emerge.

3. Emission potential

The literature review specifically revealed a lack of knowledge about emission quantities for particulate AMS emissions. To get an impression of the magnitude of particulate AMS emissions, a first emission potential for coatings of OWFs has been elaborated and presented in Section 3. The used materials and methods are described in this section. A set of maps was compiled which shows the temporal evolution of OWF emission potential in Northern Europe and Asia based on the data provided by the *Global Energy Monitor* (GEM) (Global Energy Monitor, 2023). The *Light Gray Canvas* map by Esri was used as background map (Esri, *Light Gray Canvas [Basemap]*, 2011). The GEM data provides the location of all wind farms, both onshore and offshore, as coordinates of the centroid of the wind farm. Additionally, the start year of operation for each farm is given (provided that the project has an announced start date) as well as the current status of operation, installed capacity, and the installation type (*onshore*, *offshore hard mount*, *offshore floating*, *offshore unknown*, *unknown*). Only OWFs with an announced start year are displayed starting 2024 until the year 2035. The data with 27,423 entries was filtered by year and installation type, by omitting all wind farms with an *onshore* or *unknown* installation and omitting all wind farms with an *unknown* start year, leading to a total of 765 OWFs after filtering. Additionally, cancelled projects were excluded from the analysis. It should be noted that some onshore wind parks are mislabelled as OWFs, but due to the size of the data set with 765 entries, not every single OWF could be checked manually. Furthermore, some wind parks are built in lakes on offshore-like mounts, which are also occurring in the final filtered data. Since emission potential is calculated for every single OWF separately, these outliers do not compromise the overall quality of the OWF emission calculations.

To estimate coating emissions from the OWFs, data on monopile foundation dimensions from Sánchez et al. (2019) was used to estimate the coated area per single foundation. To get the dimensions for future installations, the monopile dimensions turbine capacities from Sánchez et al. (2019) were extrapolated with the use of a least squares polynomial fit. The plots for the fitted polynomials are shown in the

Appendix (6, 6, 6). For the foundation diameter and total length, a linear fit lead to satisfying results with $r^2 = 0.72$ and $r^2 = 0.92$. For the turbine capacity, a second order polynomial was necessary to achieve a good fit with $r^2 = 0.86$. To calculate the total coated area per wind park, the number of turbines per park was estimated as well. The GEM data provides the installed park capacity of an OWF, but does not give an indication how many turbines are installed per park. Therefore, the total number of turbines was estimated based on the extrapolated turbine capacity, using the following equation: $Turbines = \frac{Capacity_{park}}{Capacity_{turbine}}$. The total coated area was determined per park and used to determine a total coating volume per OWF. A uniform coating thickness of 500 μm was used as a realistic value for an OWF coating system (Momber and Marquardt, 2018). Coating emission rates were based on a damage report from Momber (2016), who found that most coating damages are small damages with a failure rate of up to 5 %. Therefore, two emission scenarios (a low and a high scenario) are displayed for an estimated coating failure rate of 1 % and a failure rate of 5 % of the total coated area per wind park.

In the next years, the installed capacity of offshore wind will increase significantly. The temporal development of the installed capacity until 2035 can be found in the Appendix (C.13,C.14). By the end of 2024, a capacity of 100 GW will be installed. Until the end of 2030 the installed capacity is expected to increase up to 425 GW and until 2035 the capacity will increase further up to 490 GW. A first big leap in OWF construction happens between 2024 and 2030 with 323 planned new OWFs in that time period. From 2030 until 2035 41 more OWFs are currently announced. Furthermore, the new wind parks will have larger capacities which exceed the 5 GW mark, which will result in more turbines per park and larger constructions. More and larger offshore structures lead to a larger coated area and potentially more coating emissions. From the global overview, it is apparent that most of the expansion will happen in Northern Europe and Asia. Furthermore, additional wind farms are announced for the coasts of North and South America and Australia. The emission potential for Europe and Asia is displayed in Fig. 8. Each dot represents an OWF and the colour indicates the emitted coating from the structure for a low emission scenario, where 1 % of the total coated are emitted, and a high emissions scenario with a loss of 5 %.

For instance, in the low emission scenario a wind park started in 2020 with an installed capacity of 250 MW emits approximately 430 kg during its lifetime and approximately 2200 kg during its lifetime with a 5 % failure rate. To obtain the annual emission rate, the lifetime emissions of the structures were divided by their expected operational time. Assumed that an OWF is operational for 25 years and the emission rate remains linear, this would translate to annual emissions of 17.2 kg a^{-1} and 88 kg a^{-1} , respectively, for the high and low emission scenario. For all OWFs built in the Northern European area until the end of 2024 a total of 69 t (2.8 t a^{-1}) would be emitted with the lower failure rate and 345 t (13.8 t a^{-1}) for the high emission scenario. The temporal development of the coating emissions for Europe and Asia is shown in Fig. 9. Due to the significant increase in installed offshore wind capacity in the next years, the cumulative emissions for the Northern European area could increase up to 276 t (11 t a^{-1}) for an estimated failure rate of 1 % or even 1383 t (55.3 t a^{-1}) at an estimated failure rate of 5 % for all OWFs commissioned until end of 2035. For the Asian OWFs a similar trend is observable: OWFs installed until the end of 2024 have approximate cumulative emissions of 91 t (3.6 t a^{-1}) in the low emission scenario and 456 t (18.2 t a^{-1}) in the high emission scenario. Until the end of 2035 it can be expected that these emissions increase up to 190 t (7.6 t a^{-1}) and 953 t (38.1 t a^{-1}), respectively. For all wind farms around the globe that are installed latest by the end of 2024, a total of 166 t (6.6 t a^{-1}) of coating particles are emitted in the case of 1 % failure rate and 832 t (33.3 t a^{-1}) of emissions in the 5 % scenario. In 2035, all installed OWFs could potentially emit 610 t (24.4 t a^{-1}) of

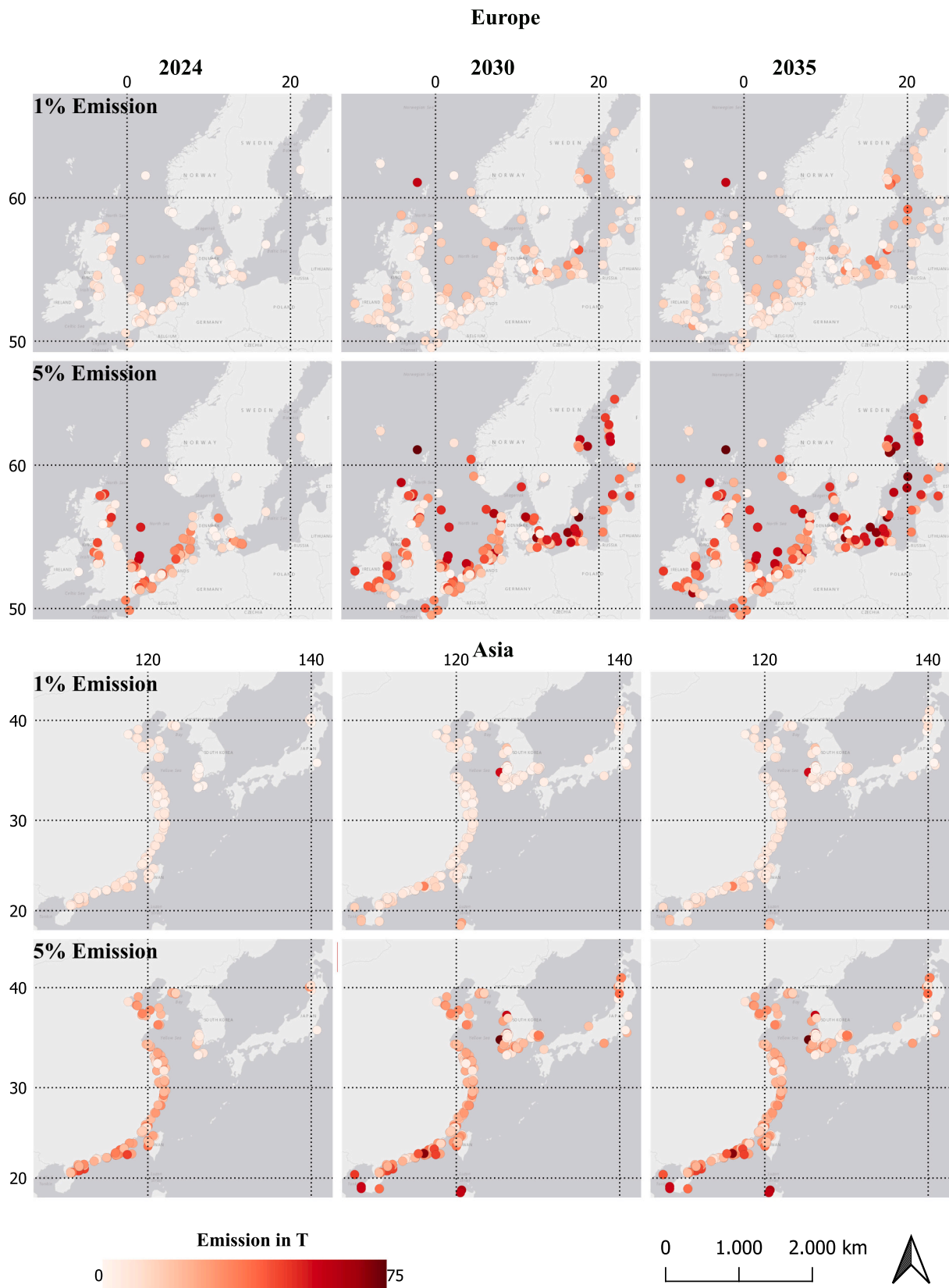


Fig. 8. Potential coating emissions per wind park for Europe and Asia. The temporal development of the emission potential is displayed for the years 2024, 2030, and 2035 as well as two different emissions scenarios with 1 % or 5 % of the total coated area emitted over the lifetime of a structure. Sources: Basemap by *Esri* and wind park data by *Global Energy Monitor* (*Global Energy Monitor, 2023; Esri, Light Gray Canvas [Basemap], 2011*).

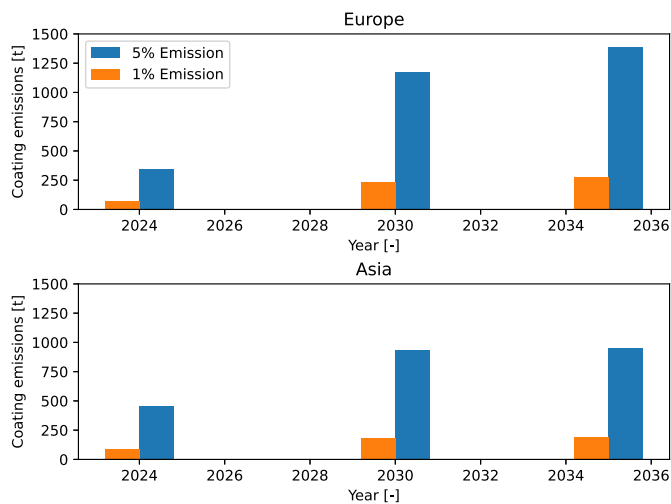


Fig. 9. Temporal development of the cumulative coating emissions for Europe and Asia. The cumulative emissions were obtained by adding all potential emissions over the lifetime of all OWFs in the respective area.

coating in the low emission scenario and 3052 t (122 t a^{-1}) of coating in the high emission scenario.

From these estimations, it is evident that the emissions caused by AMS will increase significantly, solely through the expansion of offshore wind. Based on the aforementioned estimations, the emitted coating will increase by 444 t - 2220 t globally until the end of 2035 and by 207 t - 1038 t alone in the European area. Therefore, it is of utmost importance to investigate the environmental fate and transport of particulate offshore emission further, to gather knowledge about their distribution in oceanic waters.

Since the publication by [Sánchez et al. \(2019\)](#) on the temporal development of foundation dimensions was based on monopile foundations, the simplifying assumption was made that all OWFs are built on monopile foundations. Other foundation types (e.g. jacket foundations, floating foundations) are more complex and might differ in coated area, i.e., increase their coated area significantly. For example, a monopile foundation for a 5.2 MW has a total coated area of 1480 m² whereas a floating spar-buoy which supports a 5 MW turbine has a coated area of 3675 m². Therefore, floating offshore wind can be an amplifying factor for particulate coating emissions from OWFs.

Furthermore, geometrical properties and capacity of the wind turbines are based on an extrapolation of yearly averages, which could, in reality, develop differently than the here predicted trends. Furthermore, the emission potential was calculated for fixed percentages of detaching coating without consideration of a steady release of time. The coating will deteriorate over time and detach over the lifetime of an OWF. With more data on the temporal detachment behaviour and measured quantities of detached coating, the estimations can be improved as well.

In addition to the previously mentioned limitations, the estimations presented here are performed with the implication that all future OWFs are finished on time in the intended year. Cancellation or delays of OWF installations can not be taken into account at this stage. Furthermore, only future OWFs with an already announced start date are considered in this calculation. The GEM data includes numerous OWFs which have no start year, which are excluded from the calculations, although some of these OWFs might be constructed until 2035.

Since the GEM data does not provide exact amounts of installed turbines per OWF and the exact geometrical properties, turbine numbers per park and turbine sizes were estimated by extrapolation of yearly averages from data provided by [Sánchez et al. \(2019\)](#), which is also a possible source of error. To improve the estimation, data on the exact geometrical properties of all installed OWTs would be needed.

All in all, the presented data gives a first estimation on expectable

coating emissions, which is a valuable first step towards in-depth understanding of coating emissions.

4. Conclusion

AMS are sources for particle emissions and the ambitious expansion of offshore wind in the next years will add to the numbers of AMS, amplifying the amounts of particle emissions at sea. With the operation of artificial structures in the offshore environment, particulate emissions enter the marine waters due to delaminating corrosion protection coating or other detaching material (e.g. material from OWF rotor blades). After detachment, the particles sink and get distributed in the vicinity of the structure. Once the particles have reached the seabed, they either get transported by morphodynamics, or get incorporated into deeper sediment layers, making the sediment the final sink of detached OWF particles. The main findings of this work are:

- AMS are sources for particle emissions due to delaminating corrosion protection coatings or erosion of rotor blades
- The environmental fate of particulate AMS emissions is determined by numerous processes such as sinking, remobilisation, weathering, biofouling, and morphodynamic transport and the interaction thereof
- Particle emissions will increase in the next years due to largely increasing numbers of AMS

Whilst a comprehensive knowledge of the environmental transport processes is of utmost importance to mitigate existing emissions, a reduction of particulate emissions should also be prioritised for future and existing installations. The research may have further implications, in particular with respect to the current managerial practices during installation, operation and decommissioning. This could mean that additional protection measures are implemented with respect to the handling of coated steel during installation process. Furthermore, it is essential to ensure that every installation and/or maintenance step is carefully prepared and awareness of transport and maintenance crews is increased when interacting with coated steel surfaces, which can contribute to a prolongation of the coating lifespan. Furthermore, protection measures of gear that has the potential of damaging coated steel surfaces offshore could be implemented, or coating protectors could be directly applied to commonly damaged areas, to reduce coating deterioration as well.

The processes described in the present work are mostly based on investigation results on MP particles, which are a part of the particulate AMS emissions but will not cover all sizes of emitted particles. To assess AMS emissions properly, more research on the fate and transport of particulate AMS emissions above MP size is needed. Therefore, several items for future work were identified:

- Investigation of the sinking and remobilisation behaviour of flat particles with a diameter > 5 mm
- Investigation of the influence of currents and waves on the distribution of particles around AMS foundations
- Investigation of the interaction of sediment and particles in the flow field around AMS foundations

Theoretically, the quantification of particle matter as a result of increased offshore wind activities calls for future measures that will allow a deeper insight into the described emissions. Further research is required concerning the quantification, observation and fate of particle transport originating from corrosion protection systems. Additionally, the development of crack and fail-resistant coatings with lesser deterioration rates is a promising strategy for the reduction of emissions.

The distribution of particles around offshore structures is a complex problem which requires further attention in future research. The gained knowledge will help to improve the environmental impact of said

structures further and will ultimately help to maintain a good water quality in the oceans.

CRedit authorship contribution statement

Niklas Czerner: Writing – original draft, Visualization, Data curation, Conceptualization. **Christian Windt:** Writing – review & editing, Supervision, Project administration, Conceptualization. **Nils Goseberg:** Writing – review & editing, Supervision, Project administration, Funding acquisition, Conceptualization.

Declaration of competing interest

The authors declare that they have no known competing financial interest.

Acknowledgements

We gratefully acknowledge funding through the project Anemoi (Project number 41-2-13-22), an Interreg North Sea project co-funded by the European Union.

Appendix A. Search strings for the literature review

The search strings which were used for the literature review are shown in Table A.1. The number of obtained results in both Google Scholar and Scopus™ are presented. In the course of the literature research, important keywords were identified and added to the search, leading to a wide array of search strings used in this work.

Table A.1
Search strings used for the literature review and the corresponding number of results in Google Scholar and Scopus™. Last assessed: 09.08.2024.

Search string	Results Google Scholar	Results Scopus™
offshore AND wind AND coating	40,600	210
offshore AND wind AND coating AND emissions	19,700	9
offshore AND structure AND coating AND emission	28,400	33
offshore AND structure AND coating	111,000	996
offshore AND structure AND coating AND damage	50,000	101
coating AND emission AND transport	1,600,000	1116
leading AND edge AND erosion	1,150,000	1215
microplastic AND particle AND settling AND velocity	15,200	82
microplastic AND particle AND sinking AND velocity	8980	37
microplastic AND incipient AND motion	541	4
microplastic AND remobilisation	232	12
microplastic AND particle AND remobilisation	1220	8
horseshoe AND vortex	34,400	2297
microplastic AND sediment AND transport	30,100	627
microplastic AND settling AND biofouling	7080	23
microplastic AND bioturbation	2260	53
marine AND snow AND microplastic	7910	35

Appendix B. Extrapolation plots

Figs. B.10, B.11, and B.12 show the polynomials of the extrapolated monopile data from Sánchez et al. (2019). The foundation diameter, foundation length, and turbine capacity are shown. The monopile data was extrapolated using a first order least squares polynomial fit for the foundation length and foundation diameter, and a second order least squares polynomial fit for the turbine capacity.

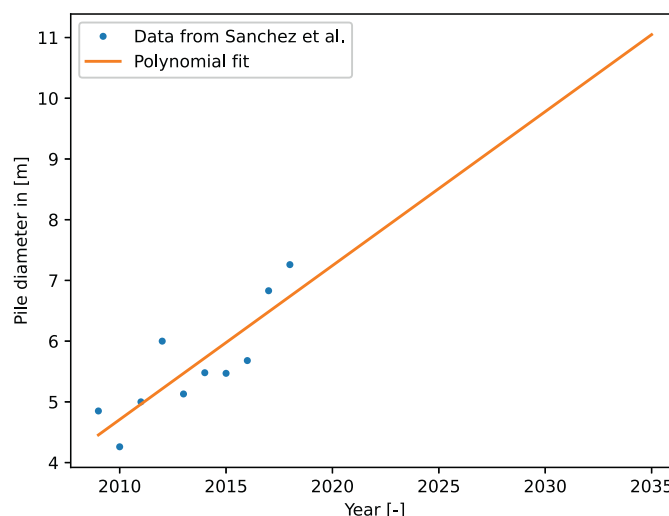


Fig. B.10. Least squares polynomial fit ($r^2 = 0.72$) of the monopile foundation diameter compiled by Sánchez et al. (2019).

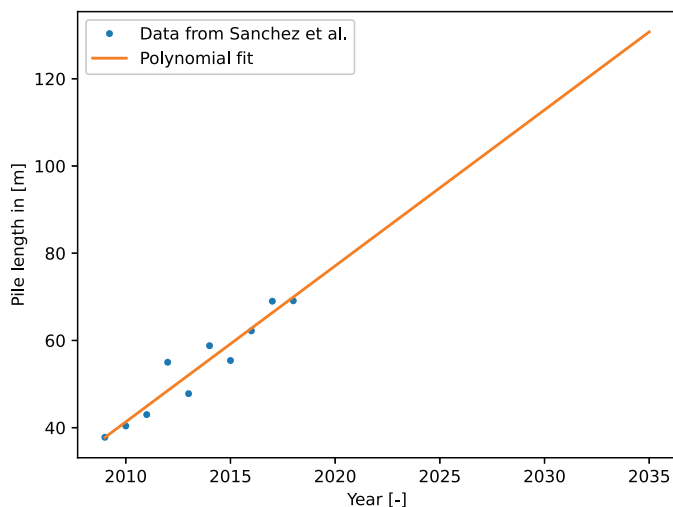


Fig. B.11. Least squares polynomial fit ($r^2 = 0.92$) of the monopile foundation length compiled by Sánchez et al. (2019).

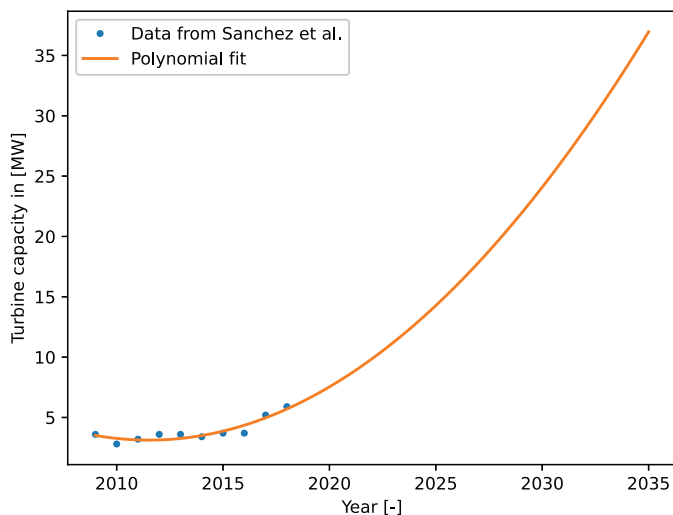


Fig. B.12. Least squares polynomial fit ($r^2 = 0.86$) of the turbine capacity compiled by Sánchez et al. (2019).

Appendix C. Temporal development of installed offshore wind capacity

Figs. C.13 and C.14 show the temporal development of the global installed capacity in offshore wind. The dots represent the centroid of an OWF and the colour indicates the installed capacity. It is evident that the number of OWFs will increase significantly, especially in Europe and Asia. Furthermore, future OWF installations will have higher installed capacities than the already existing ones.

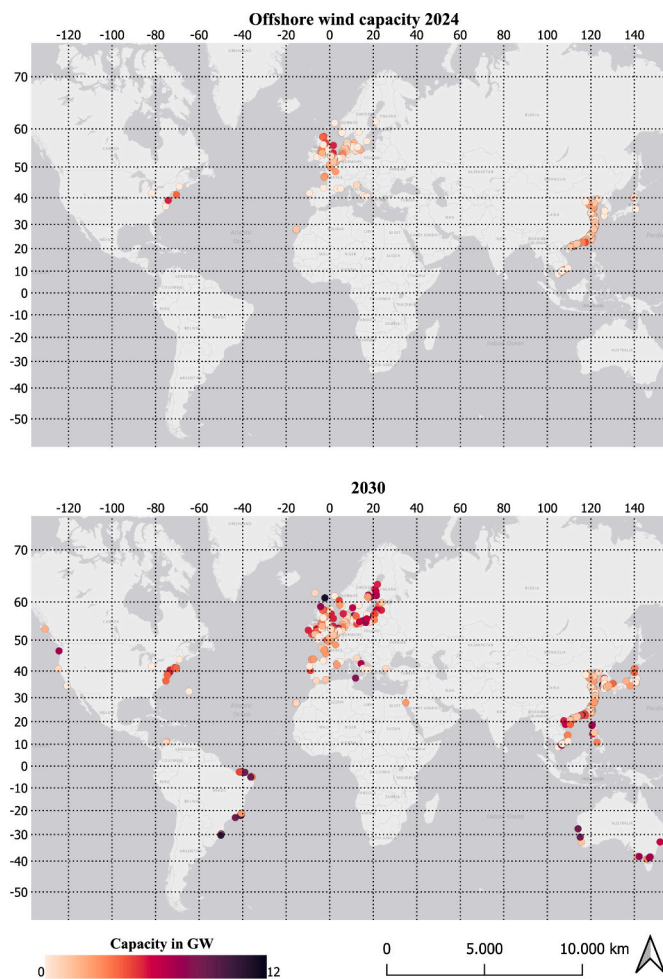


Fig. C.13. Global overview over installed wind park capacity for the years 2024 and 2030. Sources: Basemap by Esri and wind park data by Global Energy Monitor (Global Energy Monitor, 2023; Esri, Light Gray Canvas [Basemap], 2011).

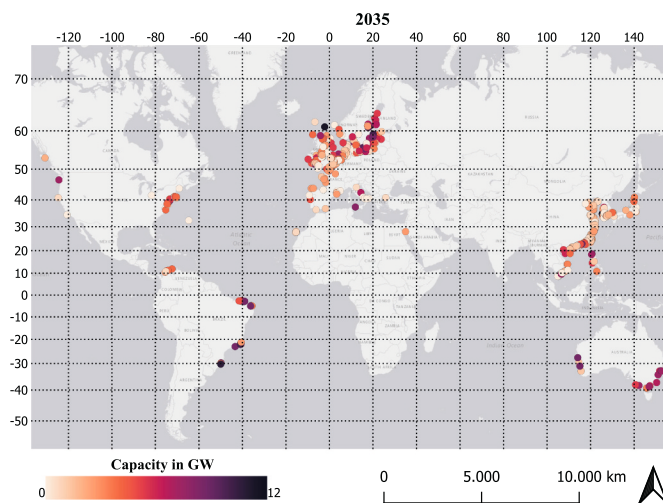


Fig. C.14. Global overview over installed wind park capacity for the year 2035. Sources: Basemap by Esri and wind park data by Global Energy Monitor (Global Energy Monitor, 2023; Esri, Light Gray Canvas [Basemap], 2011).

Data availability

Data will be made available on request.

References

Adedipe, O., Brennan, F., Kolios, A., 2016. Review of corrosion fatigue in offshore structures: present status and challenges in the offshore wind sector. *Renew. Sustain. Energy Rev.* 61, 141–154. <https://doi.org/10.1016/j.rser.2016.02.017>.

- Afzal, M.S., Holmedal, L.E., Myrhaug, D., 2021. Sediment Transport in Combined Wave–Current Seabed Boundary Layers due to Streaming. *J. Hydraul. Eng.* 147 (4), 04021007. [https://doi.org/10.1061/\(ASCE\)HY.1943-7900.0001862](https://doi.org/10.1061/(ASCE)HY.1943-7900.0001862).
- Ahmadi, P., Elagami, H., Dichgans, F., Schmidt, C., Gilfedder, B.S., Frei, S., Peiffer, S., Fleckenstein, J.H., 2022. Systematic evaluation of physical parameters affecting the terminal settling velocity of microplastic particles in lakes using CFD. *Front. Environ. Sci.* 10, 875220. <https://doi.org/10.3389/fenvs.2022.875220>.
- Aldridge, J.N., 1997. Hydrodynamic model predictions of tidal asymmetry and observed sediment transport paths in Morecambe Bay. *Estuar. Coast. Shelf Sci.* 44 (1), 39–56. <https://doi.org/10.1006/ecss.1996.0113>.
- Allredge, A.L., Silver, M.W., 1988. Characteristics, dynamics and significance of marine snow. *Prog. Oceanogr.* 20 (1), 41–82. [https://doi.org/10.1016/0079-6611\(88\)90053-5](https://doi.org/10.1016/0079-6611(88)90053-5).
- Amirzadeh, B., Louhghalam, A., Raessi, M., Tootkaboni, M., 2017. A computational framework for the analysis of rain-induced erosion in wind turbine blades, part I: stochastic rain texture model and drop impact simulations. *J. Wind Eng. Ind. Aerodyn.* 163, 33–43. <https://doi.org/10.1016/j.jweia.2016.12.006>.
- Andrady, A.L., 2011. Microplastics in the marine environment. *Mar. Pollut. Bull.* 62 (8), 1596–1605. <https://doi.org/10.1016/j.marpolbul.2011.05.030>.
- Andrady, A.L., Barnes, P.W., Bormann, J.F., Gouin, T., Madronich, S., White, C.C., Zepp, R.G., Jansen, M.A.K., 2022. Oxidation and fragmentation of plastics in a changing environment; from UV-radiation to biological degradation. *Sci. Total Environ.* 851 (Pt 2), 158022. <https://doi.org/10.1016/j.scitotenv.2022.158022>.
- Archambault, É., Campbell, D., Gingras, Y., Larivière, V., 2009. Comparing bibliometric statistics obtained from the web of science and Scopus. *J. Am. Soc. Inf. Technol.* 60 (7), 1320–1326. <https://doi.org/10.1002/asi.21062>.
- Ballent, A., Pando, S., Purser, A., Juliano, M.F., Thomsen, L., 2013. Modelled transport of benthic marine microplastic pollution in the Nazaré canyon. *Biogeosciences* 10 (12), 7957–7970. <https://doi.org/10.5194/bg-10-7957-2013>.
- Bell, A.M., Baier, R., Kocher, B., Reifferscheid, G., Buchinger, S., Ternes, T., 2020. Ecotoxicological characterization of emissions from steel coatings in contact with water. *Water Res.* 173, 115525. <https://doi.org/10.1016/j.watres.2020.115525>.
- Bijker, E.W., van Hijum, E., Vellinga, P., 1976. Sand Transport by Waves. In: *American Society of Civil Engineers (Ed.), Coastal Engineering 1976*, Reston, pp. 1149–1167.
- Castritsi-Catharios, J., Neofitou, N., Vorlou, A.A., 2015. Comparison of heavy metal concentrations in fish samples from three fish farms (eastern Mediterranean) utilizing antifouling paints. *Toxicol. Environ. Chem.* 97 (1), 116–123. <https://doi.org/10.1080/02772248.2014.943226>.
- Chen Ong, M., Trygland, E., Myrhaug, D., 2017. Numerical study of seabed boundary layer flow around monopile and gravity-based wind turbine foundations. *J. Offshore Mech. Arct. Eng.* 139 (4). <https://doi.org/10.1115/1.4036208>.
- Chubarenko, I., Bagaev, A., Zobkov, M., Esiukova, E., 2016. On some physical and dynamical properties of microplastic particles in marine environment. *Mar. Pollut. Bull.* 108 (1–2), 105–112. <https://doi.org/10.1016/j.marpolbul.2016.04.048>.
- Clemente, D., Rosa-Santos, P., Taveira-Pinto, F., 2021. On the potential synergies and applications of wave energy converters: a review. *Renew. Sustain. Energy Rev.* 135, 110162. <https://doi.org/10.1016/j.rser.2020.110162>.
- Coolen, J.W.P., Vanaverbeke, J., Dannheim, J., Garcia, C., Birchenough, S.N.R., Krone, R., Beermann, J., 2022. Generalized changes of benthic communities after construction of wind farms in the southern North Sea. *J. Environ. Manage.* 315, 115173. <https://doi.org/10.1016/j.jenvman.2022.115173>.
- Coppock, R.L., Lindeque, P.K., Cole, M., Galloway, T.S., Näkki, P., Birgani, H., Richards, S., Queirós, A.M., 2021. Benthic fauna contribute to microplastic sequestration in coastal sediments. *J. Hazard. Mater.* 415, 125583. <https://doi.org/10.1016/j.jhazmat.2021.125583>.
- Dargahi, B., 1989. The turbulent flow field around a circular cylinder. *Exp. Fluids* 8 (1–2), 1–12. <https://doi.org/10.1007/BF00203058>.
- DiBenedetto, M.H., Ouellette, N.T., Koseff, J.R., 2018. Transport of anisotropic particles under waves. *J. Fluid Mech.* 837, 320–340. <https://doi.org/10.1017/jfm.2017.853>.
- DiBenedetto, M.H., Koseff, J.R., Ouellette, N.T., 2019. Orientation dynamics of nonspherical particles under surface gravity waves. *Phys. Rev. Fluids* 4 (3), 034301. <https://doi.org/10.1103/PhysRevFluids.4.034301>.
- Dietrich, W.E., 1982. Settling velocity of natural particles. *Water Resour. Res.* 18 (6), 1615–1626. <https://doi.org/10.1029/WR018i006p01615>.
- Ebeling, A., Wippermann, D., Zimmermann, T., Klein, O., Kirchgeorg, T., Weinberg, I., Hasenbein, S., Plaß, A., Pröfrock, D., 2023. Investigation of potential metal emissions from galvanic anodes in offshore wind farms into North Sea sediments. *Mar. Pollut. Bull.* 194 (Pt A), 115396. <https://doi.org/10.1016/j.marpolbul.2023.115396>.
- Efimova, I., Bagaeva, M., Bagaev, A., Kileso, A., Chubarenko, I.P., 2018. Secondary microplastics generation in the sea swash zone with coarse bottom sediments: laboratory experiments. *Front. Mar. Sci.* 5, 402880. <https://doi.org/10.3389/fmars.2018.00313>.
- Eklund, B., Johansson, L., Ytreberg, E., 2014. Contamination of a boatyard for maintenance of pleasure boats. *J. Soil. Sediment.* 14 (5), 955–967. <https://doi.org/10.1007/s11368-013-0828-6>.
- Erdogan, C., Swain, G., 2021. Conceptual sacrificial anode cathodic protection design for offshore wind monopiles. *Ocean Eng.* 235, 109339. <https://doi.org/10.1016/j.oceaneng.2021.109339>.
- Esri, Light Gray Canvas [Basemap], 2011. Scale not provided. Retrieved July 16, 2024, from <https://www.arcgis.com/home/item.html?id=8b3d38c0819547faa83f7b7aca80bd76#overview>.
- Wind Europe, 2021. *Offshore Wind in Europe: Key Trends and Statistics 2020*, Brussels, Belgium.
- European Commission, 2022. *Annual Report on the Safety of Offshore Oil and Gas Operations in the European Union for the Year 2020*, Brussels, Belgium.
- Ferreira, V.G., Rosa, J., Almeida, N.M., Pereira, J.S., Sabater, L.M., Vendramin, D., Zhu, H., Martens, K., Higuti, J., 2023. A comparison of three main scientific literature databases using a search in aquatic ecology. *Hydrobiologia* 850 (6), 1477–1486. <https://doi.org/10.1007/s10750-022-05067-5>.
- Francalanci, S., Paris, E., Solari, L., 2021. On the prediction of settling velocity for plastic particles of different shapes. *Environ. Pollut. (Barking, Essex: 1987)* 290, 118068. <https://doi.org/10.1016/j.envpol.2021.118068>.
- Fraser, C.I., Morrison, A.K., Hogg, A.M., Macaya, E.C., van Sebille, E., Ryan, P.G., Padovan, A., Jack, C., Valdivia, N., Waters, J.M., 2018. Antarctica's ecological isolation will be broken by storm-driven dispersal and warming. *Nat. Clim. Chang.* 8 (8), 704–708. <https://doi.org/10.1038/s41558-018-0209-7>.
- Global Energy Monitor, 2023. *Global Wind Power Tracker: December 2023 release*. Global Wind Energy Council, 2024. *Global Offshore Wind Report 2024*, Global Wind Energy Council.
- Goral, K.D., Guler, H.G., Larsen, B.E., Carstensen, S., Christensen, E.D., Kerpen, N.B., Schlurmann, T., Fuhrman, D.R., 2023a. Settling velocity of microplastic particles having regular and irregular shapes. *Environ. Res.* 228, 115783. <https://doi.org/10.1016/j.envres.2023.115783>.
- Goral, K.D., Guler, H.G., Larsen, B.E., Carstensen, S., Christensen, E.D., Kerpen, N.B., Schlurmann, T., Fuhrman, D.R., 2023b. Shields diagram and the incipient motion of microplastic particles. *Environ. Sci. Technol.* <https://doi.org/10.1021/acs.est.3c02027>.
- Gourvenec, S., Sturt, F., Reid, E., Trigos, F., 2022. Global assessment of historical, current and forecast ocean energy infrastructure: implications for marine space planning, sustainable design and end-of-engineered-life management. *Renew. Sustain. Energy Rev.* 154, 111794. <https://doi.org/10.1016/j.rser.2021.111794>.
- Greaves, P., 2020. 6 - design of offshore wind turbine blades. In: Ng, C., Ran, L. (Eds.), *Offshore Wind Farms*. Woodhead Publishing Series in Energy, Duxford and Cambridge and Kidlington, pp. 105–135. Woodhead Publishing is an imprint of Elsevier.
- Guler, H.G., Larsen, B.E., Quintana, O., Goral, K.D., Carstensen, S., Christensen, E.D., Kerpen, N.B., Schlurmann, T., Fuhrman, D.R., 2022. Experimental study of non-buoyant microplastic transport beneath breaking irregular waves on a live sediment bed. *Mar. Pollut. Bull.* 181, 113902. <https://doi.org/10.1016/j.marpolbul.2022.113902>.
- Hall, P., Davies, A.M., 2004. Modelling tidally induced sediment-transport paths over the northwest European shelf: the influence of sea-level reduction. *Ocean Dyn.* 54 (2), 126–141. <https://doi.org/10.1007/s10236-003-0070-7>.
- Herring, R., Dyer, K., Martin, F., Ward, C., 2019. The increasing importance of leading edge erosion and a review of existing protection solutions. *Renew. Sustain. Energy Rev.* 115, 109382. <https://doi.org/10.1016/j.rser.2019.109382>.
- Holmedal, L.E., Myrhaug, D., 2006. Boundary layer flow and net sediment transport beneath asymmetrical waves. *Cont. Shelf Res.* 26 (2), 252–268. <https://doi.org/10.1016/j.csr.2005.11.004>.
- Hurley, R., Woodward, J., Rothwell, J.J., 2018. Microplastic contamination of river beds significantly reduced by catchment-wide flooding. *Nat. Geosci.* 11 (4), 251–257. <https://doi.org/10.1038/s41561-018-0080-1>.
- IEA, 2022. *Renewables 2022*. IEA, Paris. <https://www.iea.org/reports/renewables-2022>. retrieved: 10.03.2023.
- Isbert, W., Lindemann, C., Lemburg, J., Littmann, M., Tegethoff, K., Goseberg, N., Durst, S., Schürenkamp, D., Buck, B.H., 2023. A conceptual basis for surveying fouling communities at exposed and protected sites at sea: feasible designs with exchangeable test bodies for in-situ biofouling collection. *Appl. Ocean Res.* 136, 103572. <https://doi.org/10.1016/j.apor.2023.103572>.
- ISO 12944-2, 2017. *Paints and varnishes — Corrosion protection of steel structures by protective paint systems — Part 2: Classification of environments*.
- ISO 12944-9, 2018. *Paints and varnishes — Corrosion protection of steel structures by protective paint systems — Part 9: Protective paint systems and laboratory performance test methods for offshore and related structures*.
- Kaiser, D., Kowalski, N., Waniek, J.J., 2017. Effects of biofouling on the sinking behavior of microplastics. *Environ. Res. Lett.* 12 (12), 124003. <https://doi.org/10.1088/1748-9326/aa8e8b>.
- Kang, J.H., Jung, H., Kim, N.Y., Kim, M., Kim, G.B., 2023. Assessing the potential marine environmental impacts of heavy metal leaching from ship cleaning residues. *Ocean Sci.* 18 (4), 1–8. <https://doi.org/10.1007/s12601-023-00122-1>.
- Kirchgeorg, T., Weinberg, I., Hörnig, M., Baier, R., Schmid, M.J., Brockmeyer, B., 2018. Emissions from corrosion protection systems of offshore wind farms: evaluation of the potential impact on the marine environment. *Mar. Pollut. Bull.* 136, 257–268. <https://doi.org/10.1016/j.marpolbul.2018.08.058>.
- Kjærside Storm, B., 2023. 12 - surface protection and coatings for wind turbine rotor blades. In: Brondsted, P. (Ed.), *Advances in Wind Turbine Blade Design and Materials*. Elsevier Science & Technology, San Diego, pp. 417–440.
- Klijnstra, J., Zhang, X., van der Putten, S., Röckmann, C., 2017. Technical risks of offshore structures. In: Buck, B.H., Langan, R. (Eds.), *Aquaculture Perspective of Multi-Use Sites in the Open Ocean*. Springer International Publishing, Cham, pp. 115–127.
- Knights, A.M., Lemasson, A.J., Firth, L.B., Bond, T., Claisse, J., Coolen, J.W.P., Copping, A., Dannheim, J., de Dominicis, M., Degraer, S., Elliott, M., Fernandes, P. G., Fowler, A.M., Frost, M., Henry, L.-A., Hicks, N., Hyder, K., Jagerroos, S., Jones, D. O.B., Love, M., Lynan, C.P., Macreadie, P.I., Marlow, J., Mavraki, N., McLean, D., Montagna, P.A., Paterson, D.M., Perrow, M., Porter, J., Russell, D.J.F., Bull, A.S., Schratzberger, M., Shipley, B., van Elden, S., Vanaverbeke, J., Want, A., Watson, S.C. L., Wilding, T.A., Somerfield, P., 2024. Developing expert scientific consensus on the environmental and societal effects of marine artificial structures prior to decommissioning. *J. Environ. Manage.* 352, 119897. <https://doi.org/10.1016/j.jenvman.2023.119897>.

- Korte, A., Windt, C., Goseberg, N., 2024. Review and assessment of the German tidal energy resource. *J. Ocean Eng. Mar. Energy* 10 (1), 239–261. <https://doi.org/10.1007/s40722-023-00309-7>.
- Li, M.Z., Amos, C.L., Heffler, D.E., 1997. Boundary layer dynamics and sediment transport under storm and non-storm conditions on the Scotian shelf. *Mar. Geol.* 141 (1–4), 157–181. [https://doi.org/10.1016/S0025-3227\(97\)00060-1](https://doi.org/10.1016/S0025-3227(97)00060-1).
- López, M., López Lilaó, A., Ribalta, C., Martínez, Y., Piña, N., Ballesteros, A., Fito, C., Koehler, K., Newton, A., Monfort, E., Viana, M., 2022. Particle release from refit operations in shipyards: exposure, toxicity and environmental implications. *Sci. Total Environ.* 804, 150216. <https://doi.org/10.1016/j.scitotenv.2021.150216>.
- López, M., López-Lilaó, A., Romero, F., Pérez-Albaladejo, E., Pinteño, R., Porte, C., Balasch, A., Eljarrat, E., Viana, M., Monfort, E., 2023. Size-resolved chemical composition and toxicity of particles released from refit operations in shipyards. *Sci. Total Environ.* 880, 163072. <https://doi.org/10.1016/j.scitotenv.2023.163072>.
- Machtinger, R., Orvieto, R., 2014. Bisphenol a, oocyte maturation, implantation, and IVF outcome: review of animal and human data. *Reprod. Biomed. Online* 29 (4), 404–410. <https://doi.org/10.1016/j.rbmo.2014.06.013>.
- Martin, J., Lusher, A., Thompson, R.C., Morley, A., 2017. The deposition and accumulation of microplastics in marine sediments and bottom water from the Irish continental shelf. *Sci. Rep.* 7 (1), 10772. <https://doi.org/10.1038/s41598-017-11079-2>.
- Mazzuoli, M., Vittori, G., Blondeaux, P., 2022. The dynamics of sliding, rolling and saltating sediments in oscillatory flows. *Eur. J. Mech. B/Fluids* 94, 246–262. <https://doi.org/10.1016/j.euromechflu.2022.03.006>.
- McIntyre, J.K., Baldwin, D.H., Meador, J.P., Scholz, N.L., 2008. Chemosensory deprivation in juvenile coho salmon exposed to dissolved copper under varying water chemistry conditions. *Environ. Sci. Technol.* 42 (4), 1352–1358. <https://doi.org/10.1021/es071603e>.
- de Mesel, I., Kerckhof, F., Norro, A., Rumes, B., Degraer, S., 2015. Succession and seasonal dynamics of the epifauna community on offshore wind farm foundations and their role as stepping stones for non-indigenous species. *Hydrobiologia* 756 (1), 37–50. <https://doi.org/10.1007/s10750-014-2157-1>.
- Momber, A.W., 2016. Quantitative performance assessment of corrosion protection systems for offshore wind power transmission platforms. *Renew. Energy* 94, 314–327. <https://doi.org/10.1016/j.renene.2016.03.059>.
- Momber, A.W., Marquardt, T., 2018. Protective coatings for offshore wind energy devices (OWEAs): a review. *J. Coat. Technol. Res.* 15 (1), 13–40. <https://doi.org/10.1007/s11998-017-9979-5>.
- Momber, A.W., Plagemann, P., Stenzel, V., 2015. Performance and integrity of protective coating systems for offshore wind power structures after three years under offshore site conditions. *Renew. Energy* 74, 606–617. <https://doi.org/10.1016/j.renene.2014.08.047>.
- Muthukumar, T., Aravinthan, A., Lakshmi, K., Venkatesan, R., Vedaprakash, L., Doble, M., 2011. Fouling and stability of polymers and composites in marine environment. *Int. Biodeter. Biodegr.* 65 (2), 276–284. <https://doi.org/10.1016/j.ibiod.2010.11.012>.
- Näkki, P., Setälä, O., Lehtiniemi, M., 2017. Bioturbation transports secondary microplastics to deeper layers in soft marine sediments of the northern Baltic Sea. *Mar. Pollut. Bull.* 119 (1), 255–261. <https://doi.org/10.1016/j.marpolbul.2017.03.065>.
- Näkki, P., Setälä, O., Lehtiniemi, M., 2019. Seafloor sediments as microplastic sinks in the northern Baltic Sea - negligible upward transport of buried microplastics by bioturbation. *Environ. Pollut. (Barking, Essex: 1987)* 249, 74–81. <https://doi.org/10.1016/j.envpol.2019.02.099>.
- Nelms, S.E., Galloway, T.S., Godley, B.J., Jarvis, D.S., Lindeque, P.K., 2018. Investigating microplastic trophic transfer in marine top predators. *Environ. Pollut. (Barking, Essex: 1987)* 238, 999–1007. <https://doi.org/10.1016/j.envpol.2018.02.016>.
- Nguyen, T.H., Tang, F.H.M., Maggi, F., 2020. Sinking of microbial-associated microplastics in natural waters. *PLoS One* 15 (2), e0228209. <https://doi.org/10.1371/journal.pone.0228209>.
- Nielsen, A.W., Sumer, B.M., Fredsoe, J., Christensen, E.D., 2012. Scour Protection around Offshore Wind Turbines: Monopiles. American Society of Civil Engineers. [https://doi.org/10.1061/41147\(392\)42](https://doi.org/10.1061/41147(392)42).
- Olajire, A.A., 2018. Recent advances on organic coating system technologies for corrosion protection of offshore metallic structures. *J. Mol. Liq.* 269, 572–606. <https://doi.org/10.1016/j.molliq.2018.08.053>.
- Paoletta, G., Fabbriano, M., Locascio, A., Sirakov, M., Pontoni, L., 2024. Fate of bisphenol a in marine environment: a critical review. *Chem. Eng. J.* 495, 153228. <https://doi.org/10.1016/j.cej.2024.153228>.
- Paruta, P., Pucino, M., Boucher, J., 2021. *Plastic Paints the Environment, EA - Environmental Action, Lausanne, Switzerland*.
- Pedersen, M.L., Ullusoy, B., Weinell, C.E., Zilsteroff, F.B., Li, S., Dam-Johansen, K., 2023. CoaST maritime test Centre: an investigation of biofouling propensity. *J. Coat. Technol. Res.* 20 (3), 857–868. <https://doi.org/10.1007/s11998-022-00707-w>.
- Porter, A., Lyons, B.P., Galloway, T.S., Lewis, C., 2018. Role of marine snows in microplastic fate and bioavailability. *Environ. Sci. Technol.* 52 (12), 7111–7119. <https://doi.org/10.1021/acs.est.8b01000>.
- Provencher, J.F., Bond, A.L., Hedd, A., Montevecchi, W.A., Muzaffar, S.B., Courchesne, S. J., Gilchrist, H.G., Jamieson, S.E., Merkel, F.R., Falk, K., Durinck, J., Mallory, M.L., 2014. Prevalence of marine debris in marine birds from the North Atlantic. *Mar. Pollut. Bull.* 84 (1–2), 411–417. <https://doi.org/10.1016/j.marpolbul.2014.04.044>.
- Rachidi, F., Rubinstein, M., Smorgonskiy, A., 2012. Lightning Protection of Large Wind-Turbine Blades, in: *Wind Energy Conversion Systems*. Springer, London, pp. 227–241.
- Reese, A., Voigt, N., Zimmermann, T., Irrgeher, J., Pröfrock, D., 2020. Characterization of alloying components in galvanic anodes as potential environmental tracers for heavy metal emissions from offshore wind structures. *Chemosphere* 257, 127182. <https://doi.org/10.1016/j.chemosphere.2020.127182>.
- Rempel, L., 2012. Rotor blade leading edge erosion - real life experiences. *Wind Syst. Mag.* 2012 (October), 22–24.
- Rodrigues, M.P.M.C., Costa, M.R.N., Mendes, A.M., Eusébio Marques, M.I., 2000. Effectiveness of surface coatings to protect reinforced concrete in marine environments. *Mater. Struct.* 33 (10), 618–626. <https://doi.org/10.1007/BF02480601>.
- Rosu, L., Cascaval, C.N., Ciobanu, C., Rosu, D., Ion, E.D., Morosanu, C., Enachescu, M., 2005. Effect of UV radiation on the semi-interpenetrating polymer networks based on polyurethane and epoxy maleate of bisphenol a. *J. Photochem. Photobiol. A Chem.* 169 (2), 177–185. <https://doi.org/10.1016/j.jphotochem.2004.06.008>.
- Sadati, S., Arezoumandi, M., Shekarchi, M., 2015. Long-term performance of concrete surface coatings in soil exposure of marine environments. *Construct. Build Mater.* 94, 656–663. <https://doi.org/10.1016/j.conbuildmat.2015.07.094>.
- Salimi-Tarazouj, A., Hsu, T.-J., Traykovski, P., Chauchat, J., 2024. Investigating wave shape effect on sediment transport over migrating ripples using an eulerian two-phase model. *Coast. Eng.* 189, 104470. <https://doi.org/10.1016/j.coastaleng.2024.104470>.
- Samborsky, D.D., Wilson, T.J., Agastra, P., Mandell, J.F., 2008. Delamination at thick ply drops in carbon and glass Fiber laminates under fatigue loading. *J. Sol. Energy Eng.* 130 (3). <https://doi.org/10.1115/1.2931496>.
- Sánchez, S., López-Gutiérrez, J.-S., Negro, V., Esteban, M.D., 2019. Foundations in offshore wind farms: evolution, characteristics and range of use. Analysis of Main dimensional parameters in Monopile foundations. *J. Mar. Sci. Eng.* 7 (12), 441. <https://doi.org/10.3390/jmse7120441>.
- Sardain, A., Sardain, E., Leung, B., 2019. Global forecasts of shipping traffic and biological invasions to 2050. *Nat. Sustain.* 2 (4), 274–282. <https://doi.org/10.1038/s41893-019-0245-y>.
- Schendel, A., Goseberg, N., Schlurmann, T., 2016. Erosion stability of wide-graded quarry-stone material under unidirectional current. *J. Waterw. Port Coast. Ocean Eng.* 142 (3), 04015023. [https://doi.org/10.1061/\(ASCE\)JWW.1943-5460.0000321](https://doi.org/10.1061/(ASCE)JWW.1943-5460.0000321).
- Schendel, A., Goseberg, N., Schlurmann, T., 2018. Influence of reversing currents on the erosion stability and bed degradation of widely graded grain material. *Int. J. Sediment Res.* 33 (1), 68–83. <https://doi.org/10.1016/j.ijsrc.2017.07.002>.
- Schlichting, H., Gersten, K., 2017. *Boundary-Layer Theory*. Springer Berlin Heidelberg, Berlin, Heidelberg. <https://doi.org/10.1007/978-3-662-52919-5>.
- Schultz, M.P., 2007. Effects of coating roughness and biofouling on ship resistance and powering. *Biofouling* 23 (5–6), 331–341. <https://doi.org/10.1080/08927010701461974>.
- Shetty, C., Priyaa, A., 2022. A review on tidal energy technologies. *Mater. Today: Proc.* 56, 2774–2779. <https://doi.org/10.1016/j.matpr.2021.10.020>.
- Shields, A., 1936. *Application of Similarity Principles and Turbulence Research to Bed-load Movement*. CalTech library.
- Shohag, M.A.S., Hammel, E.C., Olawale, D.O., Okoli, O.I., 2017. Damage mitigation techniques in wind turbine blades: a review. *Wind Eng.* 41 (3), 185–210. <https://doi.org/10.1177/0309524X17706862>.
- Shojaei, B., Najafi, M., Yazdanbakhsh, A., Abtahi, M., Zhang, C., 2021. A review on the applications of polyurea in the construction industry. *Polym. Adv. Technol.* 32 (8), 2797–2812. <https://doi.org/10.1002/pat.5277>.
- Slot, H.M., Gelinck, E., Rentrop, C., van der Heide, E., 2015. Leading edge erosion of coated wind turbine blades: review of coating life models. *Renew. Energy* 80, 837–848. <https://doi.org/10.1016/j.renene.2015.02.036>.
- Song, Y.K., Hong, S.H., Jang, M., Han, G.M., Shim, W.J., 2015. Occurrence and distribution of microplastics in the sea surface microlayer in Jinhae Bay, South Korea. *Arch. Environ. Contam. Toxicol.* 69 (3), 279–287. <https://doi.org/10.1007/s00244-015-0209-9>.
- Soulsby, R.L., 1987. *The Relative Contributions of Waves and Tidal Currents to Marine Sediment Transport*. Hydraulics Research Wallingford.
- van der Stap, T., Coolen, J.W.P., Lindeboom, H.J., 2016. Marine fouling assemblages on offshore gas platforms in the southern North Sea: effects of depth and distance from shore on biodiversity. *PLoS One* 11 (1), e0146324. <https://doi.org/10.1371/journal.pone.0146324>.
- Stiess, M., 2009. *Mechanische Verfahrenstechnik - Partikeltechnologie 1*, 3rd edition. Springer-Lehrbuch, Springer, Berlin and Heidelberg. <https://doi.org/10.1007/978-3-540-32552-9>.
- Stokes, G.G., 1847. *On the Theory of Oscillatory Waves*.
- Stringham, G.E., Simons, D.B., Guy, H.P., 1969. The behavior of large particles falling in quiescent liquids. <https://doi.org/10.3133/pp562C>.
- Sumer, B.M., Christiansen, N., Fredsøe, J., 1997. The horseshoe vortex and vortex shedding around a vertical wall-mounted cylinder exposed to waves. *J. Fluid Mech.* 332, 41–70. <https://doi.org/10.1017/S0022112096003898>.
- The SET, 2022. *Plan Implementation Working Group for Offshore Wind, 2nd SET Plan; Implementation Plan for Offshore Wind*.
- Turner, A., 2021. Paint particles in the marine environment: an overlooked component of microplastics. *Water Research X* 12, 100110. <https://doi.org/10.1016/j.wroa.2021.100110>.
- Turner, A., Barrett, M., Brown, M.T., 2009. Processing of antifouling paint particles by *Mytilus edulis*. *Environ. Pollut. (Barking, Essex: 1987)* 157 (1), 215–220. <https://doi.org/10.1016/j.envpol.2008.07.001>.
- US Army Corps of Engineers, 2003. *Coastal Engineering Manual - Appendix A Glossary of Coastal Terminology*. USACE.
- Verma, A.S., Yan, J., Hu, W., Jiang, Z., Shi, W., Teuwen, J.J., 2023. A review of impact loads on composite wind turbine blades: impact threats and classification. *Renew. Sustain. Energy Rev.* 178, 113261. <https://doi.org/10.1016/j.rser.2023.113261>.

- Videla, H.A., Characklis, W.G., 1992. Biofouling and microbially influenced corrosion. *Int. Biodeter. Biodegr.* 29 (3–4), 195–212. [https://doi.org/10.1016/0964-8305\(92\)90044-O](https://doi.org/10.1016/0964-8305(92)90044-O).
- Voet, H.E.E., van Colen, C., Vanaverbeke, J., 2022. Climate change effects on the ecophysiology and ecological functioning of an offshore wind farm artificial hard substrate community. *Sci. Total Environ.* 810, 152194. <https://doi.org/10.1016/j.scitotenv.2021.152194>.
- Waldschläger, K., Schüttrumpf, H., 2019a. Effects of particle properties on the settling and rise velocities of microplastics in freshwater under laboratory conditions. *Environ. Sci. Technol.* 53 (4), 1958–1966. <https://doi.org/10.1021/acs.est.8b06794>.
- Waldschläger, K., Schüttrumpf, H., 2019b. Erosion behavior of different microplastic particles in comparison to natural sediments. *Environ. Sci. Technol.* 53 (22), 13219–13227. <https://doi.org/10.1021/acs.est.9b05394>.
- Waldschläger, K., Lechthaler, S., Stauch, G., Schüttrumpf, H., 2020. The way of microplastic through the environment - application of the source-pathway-receptor model (review). *Sci. Total Environ.* 713, 136584. <https://doi.org/10.1016/j.scitotenv.2020.136584>.
- Wang, W., Li, W.-H., Song, L.-Y., Fan, W.-J., Liu, X.-J., Zheng, H.-B., 2018. Numerical simulation and re-design optimization of impressed current cathodic protection for an offshore platform with biofouling in seawater. *Mater. Corros.* 69 (2), 239–250. <https://doi.org/10.1002/maco.201709685>.
- Woodall, L.C., Sanchez-Vidal, A., Canals, M., Paterson, G.L.J., Coppock, R., Sleight, V., Calafat, A., Rogers, A.D., Narayanaswamy, B.E., Thompson, R.C., 2014. The deep sea is a major sink for microplastic debris. *R. Soc. Open Sci.* 1 (4), 140317. <https://doi.org/10.1098/rsos.140317>.
- Yasuda, Y., Yokoyama, S., Minowa, M., Satoh, T., 2012. Classification of lightning damage to wind turbine blades. *IEEJ Trans. Electr. Electron. Eng.* 7 (6), 559–566. <https://doi.org/10.1002/tee.21773>.
- Yokoyama, S., 2013. Lightning protection of wind turbine blades. *Electr. Pow. Syst. Res.* 94, 3–9. <https://doi.org/10.1016/j.epsr.2012.07.017>.
- Yu, Z., Yao, W., Loewen, M., Li, X., Zhang, W., 2022. Incipient motion of exposed microplastics in an Open-Channel flow. *Environ. Sci. Technol.* 56 (20), 14498–14506. <https://doi.org/10.1021/acs.est.2c04415>.
- Zheng, Y., Zhou, Y., Zhou, Y., Pan, T., Sun, L., Liu, D., 2020. Localized corrosion induced damage monitoring of large-scale RC piles using acoustic emission technique in the marine environment. *Construct. Build Mater.* 243, 118270. <https://doi.org/10.1016/j.conbuildmat.2020.118270>.
- Zupan, M., Rumes, B., Vanaverbeke, J., Degraer, S., Kerckhof, F., 2023. Long-term succession on offshore wind farms and the role of species interactions. *Diversity* 15 (2), 288. <https://doi.org/10.3390/d15020288>.